UC Berkeley
UC Berkeley Previously Published Works

Title
Review of Hybrid Methods for Deep-Penetration Neutron Transport

Permalink
https://escholarship.org/uc/item/91c500xf

Journal
Nuclear Science and Engineering, 193(10)

ISSN
0029-5639

Authors
Munk, Madicken
Slaybaugh, Rachel N

Publication Date
2019-10-03

DOI
10.1080/00295639.2019.1586273

Peer reviewed

eScholarship.org Powered by the California Digital Library
University of California

Nuclear Science and Engineering

ISSN: 0029-5639 (Print) 1943-748X (Online) Journal homepage: https://www.tandfonline.com/loi/unse20

Review of Hybrid Methods for Deep-Penetration Neutron Transport

Madicken Munk & Rachel N. Slaybaugh

To cite this article: Madicken Munk & Rachel N. Slaybaugh (2019): Review of Hybrid Methods for Deep-Penetration Neutron Transport, Nuclear Science and Engineering, DOI: 10.1080/00295639.2019.1586273

To link to this article: https://doi.org/10.1080/00295639.2019.1586273

Published online: 24 Apr 2019.

Submit your article to this journal

Article views: 19

View Crossmark data

Full Terms & Conditions of access and use can be found at
https://www.tandfonline.com/action/journalInformation?journalCode=unse20

NUCLEAR SCIENCE AND ENGINEERING
© 2019 American Nuclear Society
DOI: https://doi.org/10.1080/00295639.2019.1586273

Check for updates

Review of Hybrid Methods for Deep-Penetration Neutron Transport

Madicken Munk[a]* and Rachel N. Slaybaugh[b]

[a]*University of Illinois, Urbana-Champaign National Center for Supercomputing Applications, 1205 West Clark Street, MC-257, Urbana, Illinois 61801*
[b]*University of California, Berkeley, Nuclear Engineering Department, 4155 Etcheverry Hall, MC-1730, Berkeley, California 94720-1730*

Received December 7, 2018
Accepted for Publication February 20, 2019

Abstract — *Methods for deep-penetration radiation transport remain important for radiation shielding, nonproliferation, nuclear threat reduction, and medical applications. As these applications become more ubiquitous, the need for accurate and reliable transport methods appropriate for these systems persists. For such systems, hybrid methods often obtain reliable answers in the shortest time by leveraging the speed and uniform uncertainty distribution of a deterministic solution to bias Monte Carlo transport and reduce the variance in the solution. This work reviews the state of the art among such hybrid methods. First, we summarize variance reduction (VR) for Monte Carlo radiation transport and existing efforts to automate these techniques. Relations among VR, importance, and the adjoint solution of the neutron transport equation are then discussed. Based on this exposition, the work transitions from theory to a critical review of existing VR implementations in modern nuclear engineering software. At present, the Consistent Adjoint-Driven Importance Sampling (CADIS) and Forward-Weighted Consistent Adjoint-Driven Importance Sampling (FW-CADIS) hybrid methods are the gold standard by which to reduce the variance in problems that have deeply penetrating radiation. The CADIS and FW-CADIS methods use an adjoint scalar flux to generate VR parameters for Monte Carlo radiation transport. Additionally, efforts to incorporate angular information into VR methods for Monte Carlo are summarized. Finally, we assess various implementations of these methods and the degree to which they improve VR for their target applications.*

Keywords — *Neutron transport, hybrid methods, review, deep-penetration neutron transport, variance reduction.*

Note — *Some figures may be in color only in the electronic version.*

I. INTRODUCTION

This review aims to contextualize the state of the art in the realm of hybrid methods for deep-penetration neutral particle transport. Pertinent theoretical information relevant to this topic provides a foundation for discussion of the various efforts to implement these methods for applied problems and the degree to which those efforts succeeded.

First, a brief overview of variance reduction (VR) for Monte Carlo radiation transport is described in Sec. II. Then Sec. II.C expands on the various efforts to automate VR techniques in Monte Carlo. Section III.A follows with an introduction of the concept of importance and how that relates to VR. This section also focuses specifically on how the adjoint solution of the transport equation relates to importance.

From this point, the review transitions from theory into existing implementations of VR techniques used in modern software in the nuclear engineering community. Beginning in Sec. IV.A, a description of the Consistent Adjoint-Driven Importance Sampling (CADIS) method, which has been optimized for VR of local solutions, is presented. Next, Sec. V discusses the methods implemented to reduce the variance for global solutions.

*E-mail: mmunk2@illinois.edu

This discussion includes a description of the Forward-Weighted Consistent Adjoint-Driven Importance Sampling (FW-CADIS) method. Section VI details the efforts to incorporate angular information into VR methods for Monte Carlo. Sections IV.A. through VI each conclude with a description of the various software programs in which these methods have been implemented and the degree to which they improved the VR for their target applications.

II. MONTE CARLO VARIANCE REDUCTION

The nuclear engineering community employs Monte Carlo methods for radiation transport for a wide spectrum of application problems. Monte Carlo methods aim to emulate the transport of a particle from birth, through physical interaction, to death. This is done by randomly sampling the probabilities of various interactions that a particle could encounter (e.g., particle production, elastic and inelastic scattering, absorption, and so forth). This process of transporting a single particle is repeated many times to simulate the transport of many particles throughout the problem. When the user achieves a sufficient number of samples—or particles—in the region of interest to reach the desired statistical precision, the simulation is complete. However, this naïve approach to simulating each particle—disregarding whether it is likely to contribute to the tallied result—can be extraordinarily computationally inefficient depending on the problem. A code could waste time simulating millions of "unusable" particles and still not reach the desired statistical precision for the tally. Variance reduction techniques were developed to address this issue. In general, these techniques augment the Monte Carlo transport to more effectively contribute to a particular result while not fundamentally changing the nature of the problem being solved.

II.A. Statistical Background

Variance reduction techniques are rooted in statistics, so we begin our discussion of VR techniques with a brief primer on the statistical background relevant to Monte Carlo radiation transport. Sections II.A.1, II.A.2, and II.A.3 are summarized from Refs. 1 and 2. Monte Carlo methods transport many randomly sampled particles, and when those particles reach a region of interest, they are scored in a tally. The statistical precision of the tally reflects the total number of particles sampled in a chosen region or at a chosen surface. The reliability of the answer obtained in this region then depends on the quantity of the particles sampled in each discretization of the tally phase-space.

II.A.1. Population Statistics

In radiation transport, one desires to estimate some response in phase-space. This response is the average behavior of the physical interactions in some differential phase-space in energy, space, and time. If the probability density function $f(x)$ for the response is known exactly, then the response in dx can be calculated exactly by the true mean, or

$$\bar{x} = \int_{-\infty}^{\infty} x f(x) dx \ . \tag{1}$$

Rarely is $f(x)$ known exactly, so instead, it is sampled. Using N randomly sampled particles, the estimate of the true mean value is given as

$$\hat{x} = \frac{\sum_{i=1}^{N} x_i}{N} \ , \tag{2}$$

where x_i is the i'th event and $\hat{x}$ is the sample mean, or the estimated value of $\bar{x}$ based on the N number of samples that were used to calculate $\hat{x}$. As $N \to \infty$, $\hat{x}$ will $\to \bar{x}$, which is given by the Strong Law of Large Numbers.[2] In itself, $\hat{x}$ is a useful measure, but determining the spread of values about $\hat{x}$ is also an important measure. This is called the variance. The true variance of the distribution is

$$\sigma^2(x) = \overline{x^2} - \bar{x}^2 \ , \tag{3}$$

and the standard deviation is the square root of the variance:

$$\sigma(x) = (\overline{x^2} - \bar{x}^2)^{1/2} \ . \tag{4}$$

The variance of the sampled distribution differs, as a finite number of samples are used to calculate $\bar{x}$ and σ. The sample variance is defined by

$$S^2 = \sum_{i=1}^{N} \frac{(x_i - \hat{x})^2}{N-1} \cong \widehat{x^2} - \hat{x}^2 \ , \tag{5}$$

where

$$\widehat{x^2} = \frac{1}{N} \sum_{i=1}^{N} x_i^2 \ , \tag{6}$$

and the sample standard deviation is given by

$$S = (\widehat{x^2} - \widehat{x}^2)^{(1/2)} \ . \tag{7}$$

For Eq. (5) to hold true, the number of N samples must be large. S^2 is the sample estimate of the true variance σ^2. The variance of the estimate of the mean value about $\overline{x}$ is

$$S_{\hat{x}}^2 = \frac{S^2}{N} \ . \tag{8}$$

From Eq. (8), one can see that the relationship between the sample standard deviation and the standard error of $\widehat{x}$ about $\overline{x}$ is

$$S_{\hat{x}} = \sqrt{\frac{S^2}{N}} = \frac{S}{\sqrt{N}}, \tag{9}$$

where $S_{\widehat{x}}$ is the standard error of the estimate of the sample mean. The relative error normalizes the standard error by the estimate of the mean

$$R = \frac{S_{\hat{x}}}{\widehat{x}} \ . \tag{10}$$

As a result, S, R, and N follow the relationship

$$S^2 \propto R^2 \propto \frac{1}{N} \ . \tag{11}$$

II.A.2. The Central Limit Theorem

Suppose $\widehat{x}$ is calculated from several independent random particles to estimate $\overline{x}$. At what point does one conclude that $\widehat{x}$ sufficiently reflects $\overline{x}$? The central limit theorem[1,2] (CLT) is a very powerful supplement to the quantities described in Sec. II.A.1. The CLT states that for large N, $\widehat{x}$ will have a limiting distribution $f_N(\widehat{x})$, and that distribution will be a normal distribution

$$f_N(\widehat{x}) \approx \frac{1}{\sqrt{2\pi}\sigma(\widehat{x})} \exp\left[\frac{-(\widehat{x}-\overline{x})^2}{2\sigma^2(\widehat{x})}\right], \quad N \to \infty \ . \tag{12}$$

The standard deviation of $\widehat{x}$ can be related to the standard deviation of the samples by

$$\sigma(\widehat{x}) = \frac{\sigma(x)}{\sqrt{N}} \ . \tag{13}$$

Using the definition from Eq. (13) in Eq. (12) results in

$$f_N(\widehat{x}) \approx \sqrt{\frac{N}{2\pi}} \frac{1}{\sigma(x)} \exp\left[\frac{-N(\widehat{x}-\overline{x})^2}{2\sigma^2(x)}\right], \quad N \to \infty \ . \tag{14}$$

This allows us to use known values for $\widehat{x}$ and an approximation of $\sigma(x)$, using S, to determine the probability density function of the sample means $f_N(\widehat{x})$. Because $f_N(\widehat{x})$ is normally distributed, we can find the probability that $\widehat{x}$ lies in $\overline{x} \pm \varepsilon$ with

$$P\{\overline{x} - \varepsilon < \widehat{x} \le \overline{x} + \varepsilon\} = \int_{\overline{x}-\varepsilon}^{\overline{x}+\varepsilon} f_N(\widehat{x}) d\widehat{x} \ . \tag{15}$$

Placing our definition for the distribution of $\widehat{x}$, which is $f_N(\widehat{x})$, into Eq. (15); changing the limits of integration; and defining a new variable t such that

$$t = \sqrt{N/2}[(\widehat{x}-\overline{x})/\sigma(x)] \ , \tag{16}$$

this becomes

$$P\{\overline{x} - \varepsilon < \widehat{x} \le \overline{x} + \varepsilon\} = \frac{2}{\sqrt{\pi}} \int_0^{(\sqrt{N/2})(\varepsilon/\sigma(x))} e^{-t^2} dt \ . \tag{17}$$

Recall that the definition of the error function Eq. (17) becomes

$$P\{\overline{x} - \varepsilon < \widehat{x} \le \overline{x} + \varepsilon\} = \text{erf}\left[\sqrt{\frac{N}{2}} \frac{\varepsilon}{\sigma(x)}\right] \ . \tag{18}$$

Then, using the calculated estimation S for the true standard deviation $\sigma(x)$ and also recalling that $S_{\hat{x}} = S/\sqrt{N}$ [Eq. (9)], the error function reduces to a function of ε and $S_{\hat{x}}$, or

$$\text{erf}\left[\sqrt{\frac{N}{2}} \frac{\varepsilon}{\sigma(x)}\right] = \text{erf}\left[\sqrt{\frac{1}{2}} \frac{\varepsilon}{S_{\hat{x}}}\right] \ . \tag{19}$$

Should ε be chosen to be a function of $S_{\hat{x}}$, the error function reduces further and becomes merely an evaluation as M multiples of $S_{\hat{x}}$ and $\sqrt{1/2}$. For the first few multiples of the standard error, this is evaluated as

$$P\{\overline{x} - MS_{\hat{x}} < \widehat{x} \le \overline{x} + MS_{\widehat{x}}\} = \begin{cases} 0.683, & M = 1, \\ 0.954, & M = 2, \\ 0.997, & M = 3 \end{cases} . \tag{20}$$

The CLT tells us that the sample mean follows a normal distribution, regardless of the distribution of the underlying sample, as the number of samples approaches infinity. This means that no matter what distribution is being sampled, the sampled mean will have this expected behavior. As a result, given a calculated value for $\hat{x}$ and S, the probability that $\hat{x}$ is near $\bar{x}$ is known and calculable. Further, the CLT shows that this distribution is approached very quickly as N increases, with most problems only requiring $N > 30$ (Ref. 1). Note that N is not the total number of samples but is the number of samples required to calculate each mean.

However, for the CLT to hold, a number of requirements must be satisfied. All of the quantities in Sec. II.A.1 have the underlying assumption that each x_i is assumed to be randomly sampled and independent of other x_i. If some region of phase-space is omitted accidentally, these values will not be reflective of the true $f(x)$, and so $\hat{x}$ will not approximate $\bar{x}$. Further, for S to be a good approximation of $\sigma(x)$, a large number of N samples must contribute to the calculation of $\hat{x}$. The CLT also assumes that $f(x)$ is a probability density function that can be sampled and has a variance that exists. As a result, one must be reasonably sure that all of these requirements are satisfied if using Monte Carlo sampling methods.

II.A.3. The Figure of Merit

The equations in Secs. II.A.1 and II.A.2 describe how to estimate the statistics of a population given a finite number of samples. In radiation transport, a user seeks to estimate some response, the relative error associated with that response solution, and the time it takes to obtain those values. Equation (11) describes the relationship among the sample variance, the relative error, and the number of particles as

$$S^2 \propto R^2 \propto \frac{1}{N} .$$

The relationship between the relative error R and the number of particles N (recall that $R^2 \propto \frac{1}{N}$) will be some constant value C_1:

$$C_1 = R^2 N . \tag{21}$$

As a problem is simulated, the number of particles run N will increase proportionally to the computational transport time T. Therefore, the relationship between R and T should also be a constant:

$$C_2 = R^2 T . \tag{22}$$

The figure of merit (FOM) shown in Eq. (23) is the most commonly reported metric using this relationship. It is widely used in quantifying the effects of VR methods. Because it uses the inverse quantity of the relative error and time, a "good" result would be obtained from a low relative error in a short amount of time, resulting in a FOM with a high numerical value:

$$\text{FOM} = \frac{1}{R^2 T} . \tag{23}$$

Once the FOM for a problem has been determined, it can be used to reveal information about future computations of the problem. For example, a user may wish to determine the resultant error given a specified run time. In that case, Eq. (23) can simply be rearranged to

$$R = \frac{1}{(\text{FOM} \times T)^{1/2}} . \tag{24}$$

The FOM is a very useful tool, but it is limited by statistical precision in calculating R. Early on in a transport simulation, when too few particles have been simulated to effectively capture S or $\hat{x}$, the FOM will oscillate. Eventually, the FOM will converge to a relatively constant value. This behavior can also be used to determine whether one has sufficiently sampled the region in which he or she is quantifying the response.

II.B. Variance Reduction Methods for Monte Carlo Radiation Transport

Having introduced the key parameters affecting variance in a problem, let us transition to different VR techniques available in Monte Carlo radiation transport packages. Variance reduction techniques in radiation transport methods fall into four general categories: population control methods, modified sampling methods, truncation methods, and partially deterministic methods.

II.B.1. Population Control Methods

Population control methods adjust the particle population in the problem to obtain better sampling in regions of interest by preferentially increasing or decreasing the particle population. The first two types of population control methods that will be discussed are called splitting and rouletting. Splitting is a method by which the particle population can be increased by splitting a single higher-weight particle into several lower-weight particles. Rouletting, conversely, reduces the particle

population by stochastically killing particles. Particles that survive a rouletting routine have their weight adjusted higher, thereby conserving weight in the routine. Both splitting and rouletting maintain a fair game by adjusting the particle weights as each routine is performed; statistically, the sum of the child particle weights is the same as the parent weight as it entered the routine.

To use population control methods effectively as a VR technique, splitting is performed in high-importance regions to increase the particle count—and thus the sampling—in important regions. Conversely, rouletting is performed in low-importance regions to reduce the particle population in unimportant regions. For now, consider important regions as those that are significant to contributing to a tally result. A more thorough discussion of importance is presented in Sec. III.A. Splitting and rouletting can be applied to include space, angle, energy, and time.

The weight window combines splitting and rouletting to keep particles within a desired weight range. Figure 1 illustrates the different processes a particle may go through when passing through a weight window.

The top particle entering the weight window is a single, high-weight particle. The weight of this particle is above the weight window bounds, so as it enters the weight window, it is split into multiple particles whose weight is within the window bounds. The second particle entering the window is within the weight window bounds, so it retains its weight and is not split or rouletted. The last two particles entering the window have weights lower than the bound. They undergo a rouletting routine and one particle is killed, and the surviving particle is increased in weight. As these particles leave the window, all of them have weights within the range of the window. This will reduce the variance of the particles contributing to a tally in that region.

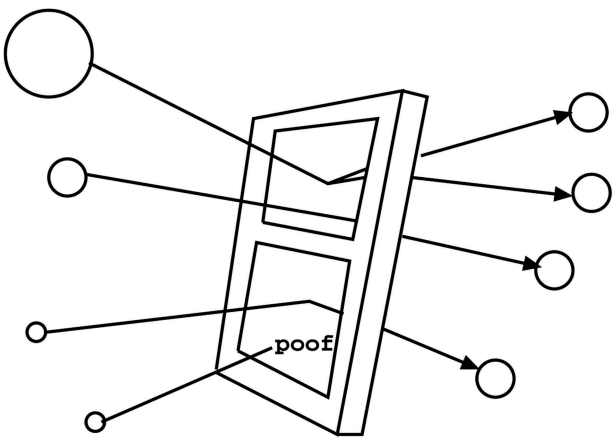

Fig. 1. Cartoon illustration of a weight window, adapted from Refs. 3 and 4.

While the use of weight windows in a problem helps to keep a more ideal distribution of particle weights, the user is faced with calculating a significant number of parameters to determine weight windows for the entire problem. In the best case with an experienced user, this may just take time. With an inexperienced user or a complex problem, this can be insurmountable and may be too difficult to do without some automated assistance.

It should be noted that while splitting and rouletting can be performed on a single variable, i.e., angle, energy, space, or time, the weight windows generally used are either energy-space dependent or space-time dependent. Further, the weight window will split or roulette depending on the particle weight entering the window. Given a cell with importance I and an adjacent cell with importance I', splitting and rouletting on their own either increase or decrease the particle weight proportional to the ratio of the cell importances, or I'/I, no matter what the entering particle weight is. As a result, poorly chosen splitting or rouletting parameters can still result in significant tally variance because particle weights may still span a wide range.

II.B.2. Modified Sampling Methods

Modified sampling methods adjust transport by sampling from a different probability distribution function than the actual distribution for the problem. This is possible if, as with population control methods, the particle weights are adjusted accordingly. The new probability distribution function should direct particles in regions of high importance to the problem tallies. In MCNP, a number of modified sampling methods exist. These include the exponential transform, implicit capture, forced collisions, source biasing, and neutron-induced photon production biasing.

The exponential transform modifies particle transport from the analog problem by artificially modifying the macroscopic cross section, and thus the distance to collision, to move particles in important directions. In directions of higher importance, the cross section is reduced and particles can flow more freely. In directions of lower importance, the cross section is increased and particles more frequently interact, thereby increasing their probability of directional change or absorption. The transformed cross section used by the exponential transform is defined by

$$\Sigma_t^* = \Sigma_t(1 - p\mu) \ , \tag{25}$$

where

Σ_t^* = transformed total macroscopic cross section

Σ_t = true total macroscopic cross section

p = transform parameter

μ = cosine of the angle between the preferred direction and the particle's transport direction.[2,4,5]

Because the particle's transport is adjusted in the exponential transform, the particle weight must be adjusted accordingly. This is given by

$$w^* = \frac{\Sigma_t e^{-\Sigma_t s}}{\Sigma_t^* e^{-\Sigma_t^* s}} = \frac{e^{-\rho\Sigma_t \mu s}}{1 - p\mu} \ , \tag{26}$$

where s is the phase-space of particle residence. This weight adjustment ensures that the particle weight is conserved throughout transport, even as the cross section is altered. Because the cross section in the problem is both energy and material dependent (depending on the geometry), the exponential transform will be dependent on space and energy, and particle transport will be augmented in both. While a powerful method, the exponential transform is quite difficult to use, and if p is ill chosen, this method can perform quite poorly. Further, the user has to know quite a bit about the problem physics and material to choose an optimal quantity for p.

Source biasing, rather than preferentially adjusting particles' directionality by way of adjusting the cross sections, biases particles from their origin. Source biasing has the option to bias particles in energy, direction, and space (if the source is volumetric). This allows the user to choose importance separately for each variable. First, the source variable is defined as a series of bins or a function. Second, the bins are assigned probabilities of occurrence according to their importance. As an illustrative example, let us consider energy for the moment. An energy bin with a high importance will be assigned a high probability of occurrence, and a bin with low importance will be assigned a low probability of occurrence. As particles are born in the bins with higher importances, they will have their weights adjusted to the inverse of their probability of occurrence, or $w^* = p/p^*$, where p refers to the probability density function for the source particles; it bears no relation to the exponential transform factor.

Source biasing is a very simple method that can reduce the solution variance significantly. However, if a user chooses bin sizes or a function that does not properly reflect the particles' importances in the problem, the source will be poorly sampled. As a result, sampling may be very inefficient, and the FOM will decrease. In MCNP, if poor parameters are chosen for this method, the user is given a warning.

II.B.3. Truncation Methods

Truncation methods stop tracking particles in a region of phase-space that is of low importance to the tally. These methods can be used in space (a vacuum boundary condition), energy (eliminate particles above or below a specified energy), or time (stop tracking after a given time). To effectively use these methods, the user must be aware of particles' importance to a tally result. When important particles are eliminated with a truncation method, the tally will lack the contribution from those particles' phase-space and will correspondingly be underestimated. Further, as discussed in Sec. II.A.2, the CLT only holds assuming that the histories tracked are independent and drawn from identical distributions. Truncating particles of high importance removes the independence from the sampling and modifies the underlying probability density function being sampled, so the estimate of the response will be invalid.

II.B.4. Partially Deterministic Methods

Partially deterministic methods typically use a deterministically calculated response function, overcoming the need for stochastic Monte Carlo in certain regions of the problem. In those regions, the probability of scattering into the region of interest is deterministically calculated and recorded by an associated tally at each step of the Monte Carlo random walk. Such methods include point tallies and forced flight methods such as Deterministic Transport[6] (DXTRAN), a method built into MCNP6. As such methods have not been proven in deep-penetration problems and instead perform best in voids,[6] they are not discussed further in this review.

It is important in using any VR technique to ensure that a fair game is being played. The user must ensure that the fundamental nature of the problem is not being changed by using a VR technique, or the answer will not

be representative of the original problem. Automated VR techniques aim to eliminate this uncertainty for the user by estimating the importance of particles in some way and then setting up VR parameters automatically. The remainder of this review paper will focus on efforts to automate population control methods and modified sampling methods for VR.

II.C. Historical Automated VR Methods for Monte Carlo Radiation Transport

Section II.B describes some methods that one may use to reduce the variance in Monte Carlo radiation transport tallies. These methods, if used correctly, can significantly increase the transport efficiency in a Monte Carlo simulation. However, correct use of these methods often requires intelligent selection of VR parameters, which is a nontrivial task. Users have found themselves often performing several trial runs before choosing final quantities for the VR parameters in their problems, which was computationally inefficient and required significant knowledge of Monte Carlo and VR to execute well.[7]

This has been addressed by using Monte Carlo to sample the problem in an initial calculation to determine more favorable VR parameters automatically. Recognizing that choosing optimal weight window values for energy- and space-dependent weight windows was difficult even for experienced users, Booth and Hendricks proposed two tools for Monte Carlo VR in parallel. The first was a Monte Carlo importance generator[7] that could be used to make informed decisions on cell importances throughout the problem. The second method, a Monte Carlo–generated weight window generator (WWG), calculates the weight window values automatically for a given problem.[8] The importance generator estimates a cell's importance by tracking the weights of the particles in the cell, or

$$\text{Importance} = \frac{\text{score of particles leaving the cell}}{\text{weight leaving the cell}} . \tag{27}$$

The WWG calculates weight window values with

$$W_{i,low} = \frac{1}{kN}\left[\sum(W_{i,in}) + \sum(W_{i,out})\right] \tag{28a}$$

and

$$W_{i,high} = \begin{cases} k \times W_{i,low} & \text{if } W_{i,low} \neq 0 \\ \infty & \text{if } W_{i,low} = 0 \end{cases} , \tag{28b}$$

where

$W_{i,low}, W_{i,high}$ = weight window lower and upper weight bounds, respectively

$\sum(W_{i,in}), \sum(W_{i,out})$ = total weight entering and leaving the cell

N = number of source particles

k = some weight window width (a constant that Hendricks[8] set to 5).

In his paper, Booth notes that the weight window target value derived from the importance generator was chosen so that the track weight multiplied by the expected score in the tally region (for unit track weight) was approximately constant. Booth's importance generator saw improvements in the FOM between 1.5 to 8 times when compared to the analog run for the test problem presented.

Booth and Hendricks combined these two methods to automate weight window generation based on phase-space importance.[9,10] They showed that the combination of the importance estimator and the WWG was a successful way to perform VR in deep-penetration problems. However, their method depended on several iterations of importance-determining runs to obtain a satisfactory estimation of the importance. For a 300-cm slab problem, the FOM was increased from 1.9 to 75 but took ten subsequent runs to obtain the FOM of 75, and these runs ranged from 1.2 min (for the analog problem) to 42 min (for the ninth run[10]).

It should be noted that both the importance generator and the WWG use a lower-fidelity Monte Carlo run to gain an initial estimate for a cell's importance and generate VR parameters from them to bias a more computationally intensive and higher-fidelity run. Naturally, the VR parameters generated by using these techniques are limited by the statistical precision in the regions used to generate them. Hendricks also pointed out that the WWG tended to populate all regions of phase-space equally, which he conceded was not ideal for all problems.[8] Furthermore, for deep-penetration particle transport, the VR parameters for low flux regions are exceedingly difficult to generate, resulting in unfavorable VR parameters.

The MCNP (Refs. 2 and 3) WWG has been extended beyond the initial space and energy implementation described in Booth's paper. It now has the ability to automatically generate space, energy, and angle weight windows. The importance generator in MCNP also has been extended to time importance, the values of which can be used for splitting or rouletting parameters[3] and can be

optimized on a grid independent from the MCNP geometry.[11]

As with the original implementations of Booth and Hendricks, this updated WWG still relies on adequate sampling to obtain sufficient weight window parameters. When additional degrees of freedom, like angle dependence, are added, the time to converge on those parameters takes even longer. The WWG also allows for only a single tally to be optimized at once, so multiple tallies cannot be optimized simultaneously. Finally, the WWG still requires user input and updating to seed the weight window solution. The user must choose the meshing of the problem and have some intuition as to how the problem should be subdivided. In the report by Van Riper and Los, it was found that depending on user experience, the WWG can have differences ranging between a factor of 2 to a factor of 10 (Ref. 12) for the problems that they investigated.

III. IMPORTANCE FUNCTIONS FOR VR

The effective use of VR techniques can lead to a faster time to a desired solution and a reduced variance in the specified tally. As noted, however, specifying VR parameters is not always a straightforward procedure. In simple geometries, a user might intuitively understand which regions of a problem may contribute more to a desired solution, but for more complex geometries, this may not be so obvious. In Secs. III.A, III.B, and III.C, the theory in determining which regions of a problem are important to eliciting a tally response will be described. The first topic discussed will be the concept of importance and obtaining a measure of importance with Monte Carlo sampling. Second, the adjoint equation and its relation to importance will be introduced. Last, the contributon solution and how it relates to tally responses is reviewed.

III.A. The Concept of Importance

The concept of importance is, in essence, a way of defining which regions in a problem are more likely to contribute to a response and which are less likely to contribute to a response. The regions that are more likely to generate a response will have a higher importance than those that do not. If an importance function for a system can be obtained computationally, that importance function can be strategically used in VR techniques to speed up the Monte Carlo calculations.

As described in Sec. II.C, Booth[7] proposed a method to quantify a cell's importance within a Monte Carlo simulation [Eq. (27)]. In this method, Booth suggested estimating the cell's importance using Monte Carlo transport as[a]

$$\text{Importance} = \frac{\text{score of particles leaving the cell}}{\text{weight leaving the cell}} .$$

This particular calculation of importance follows from the intuitive explanation for importance in the preceding paragraph. Recall from Sec. II.B that in VR methods, the population of particles is increased in important regions such that the number of samples or particles contributing to a tally increases but the total problem weight is conserved. More important regions should have many lower-weight particles to reduce the tally variance. By using Booth's bookkeeping method for estimating regional importance, and noting that in a problem with no weight variation every particle has an equal weight assumed to be unity, one can determine the relative importance of a cell. If the total score in the tally from particles leaving the cell is less than the sum of the weights of the departing particles, then the relative contribution of that cell to the tally is likely to be lower than other regions. If, instead, the total score tallied from particles leaving the cell is greater than the weight leaving the cell, then that region is more important to the tally response.

While this estimation of the importance requires only a Monte Carlo forward calculation of the problem, it is referred to as the forward-adjoint importance generator[7,9,10] because the bookkeeping tracked by Eq. (27) is a forward approximation of the adjoint. Adjoint theory and how it relates to importance will be discussed in Sec. III.B. Booth's estimation of importance was used to generate weight window target values inversely proportional to the importance. In this case, the track weight multiplied by the expected score is approximately constant in the problem. Choosing this inverse relationship between the weight window and importance is common practice in VR and is often a good choice because it is nearly optimal over a broad range of a problem phase-space.[13]

It should be noted that Booth's method is dependent on the reliability of the answers obtained in the cells to generate their importances. That is, if the cell tally has

[a] While Booth defined importance related to particles leaving the cell in Eq. [7], in a later paper with Hendricks,[10] importance was defined as related to particles and their weights entering the cell. As long as the bookkeeping remains consistent, the importance estimates should be comparable.

poor sampling and low statistical precision, the importance estimate will be equivalently poor. For deep-penetration problems, obtaining a "good" estimate of the cell importances many mean free paths from the forward source takes several iterations. With large fluctuations between iterations, this has the potential to be a very slow and computationally inefficient way to calculate importance in a problem. Using a solution of the adjoint that is equally valid across all of the problem space is more ideal for deep-penetration problems.

III.B. The Adjoint Solution for Importance

Using the solution of the adjoint formulation of the neutron transport equation is one of the most widely recognized methods for generating an importance function. This section will begin with a brief summary of adjoint theory. A discussion on how the adjoint solution differs physically from the forward solution for a particular problem follows. Last, some early investigations on how the adjoint and importance are related are summarized.

III.B.1. Theory

In Secs. II and III.A we have reviewed the statistical precision of Monte Carlo–based methods and how sampled results in Monte Carlo can be obtained in less time with VR methods. We have also briefly addressed the forward and the adjoint solutions for a particular problem. In neutron transport, the integral form of the forward, steady-state, particle transport equation can be defined as

$$\begin{aligned}&\widehat{\Omega}\cdot\nabla\psi(\vec{r},E,\widehat{\Omega})+\Sigma_t(\vec{r},E)\psi(\vec{r},E,\widehat{\Omega})=\\&\int_{4\pi}\int_0^\infty\Sigma_s(E'\rightarrow E,\widehat{\Omega}'\rightarrow\widehat{\Omega})\psi(\vec{r},E',\widehat{\Omega}')dE'\,d\widehat{\Omega}'\\&+q_e(\vec{r},E,\widehat{\Omega})\ ,\end{aligned}\tag{29}$$

where

$\vec{r}, E, \widehat{\Omega}$ = position, energy, and direction, respectively, giving six dimensions of phase-space in total

ψ = neutron flux

Σ = neutron interaction (scattering, absorption, total) cross section

q_e = external fixed source.

Alternatively, this can be written in operator form:

$$H\psi=q_e\ ,\tag{30}$$

where

H = streaming, scattering, and absorptive terms from Eq. (29)

ψ = angular flux as it is in Eq. (29)

q_e = source term.

The forward transport equation tells us where particles are moving throughout the system. Of note, the particles move in the scattering term from E' into E, and from $\widehat{\Omega}'$ into $\widehat{\Omega}$. Therefore, for a particular problem with a given q_e, particles start at q_e and move throughout the system, either scattering in energy, streaming out of the problem, being absorbed by the problem materials, or inducing a response at the tally location.

The adjoint equation of the same form, in contrast, can be expressed as

$$\begin{aligned}&-\widehat{\Omega}\cdot\nabla\psi^\dagger(\vec{r},E,\widehat{\Omega})+\Sigma_t(\vec{r},E)\psi^\dagger(\vec{r},E,\widehat{\Omega})=\\&\int_{4\pi}\int_0^\infty\Sigma_s(E\rightarrow E',\widehat{\Omega}\rightarrow\widehat{\Omega}')\psi^\dagger(\vec{r},E',\widehat{\Omega}')dE'\,d\widehat{\Omega}'\\&+q_e^\dagger(\vec{r},E,\widehat{\Omega})\ ,\end{aligned}\tag{31}$$

or in operator form as

$$H^\dagger\psi^\dagger=q_e^\dagger\ ,\tag{32}$$

where the variables with † signify the adjoint-specific variables for the problem: the adjoint flux $\psi^\dagger$ and the adjoint source $q_e^\dagger$. Note here that the particles in the adjoint equation move from E into E', and from $\widehat{\Omega}$ into $\widehat{\Omega}'$, which indicates a reversal of scattering in energy and a reversal of direction when compared to the forward problem. Therefore, if a particle has a downscattering event in energy in the forward problem, the complementary particle in the adjoint problem will have an upscattering event in energy. The external source, too, is different, changing from q_e to $q_e^\dagger$.

To solve the adjoint problem, the adjoint source $q_e^\dagger$ can be chosen such that it has the potential to reveal information about the forward problem. In Monte Carlo VR we seek to obtain information on the detector or

tally response for the system. The response for the forward problem given a defined source distribution $q(\vec{r}, E, \widehat{\Omega})$ is

$$R_{tally} = \int_{4\pi}\int_{V}\int_{E} \psi(\vec{r}, E, \widehat{\Omega})\Sigma_{tally}(\vec{r}, E, \widehat{\Omega}) dE dV d\widehat{\Omega} \ , \tag{33a}$$

where dE, dV, and $d\Omega$ are the differential spaces of energy, volume, and angle, respectively, in the tally region. This can be simplified using bracket notation, where the angle brackets indicate an integration over all phase-space:

$$R_{tally} = \langle \psi \Sigma_{tally} \rangle \ , \tag{33b}$$

where ψ is the angular flux and Σ_{tally} is the effective tally response function.

For a simple source-detector problem, we choose $q_e^{\dagger}$ to be Σ_{tally}, or the adjoint source is the tally/detector response function for the system. Therefore, the adjoint particles start at the detector location, move away from the adjoint source (the detector location), and scatter in a reversal of energy as compared to the forward problem. By making the choice that $q_e^{\dagger} = \Sigma_{tally}$, the response function can be written as a product for the forward flux and the adjoint source:

$$R_{tally} = \langle \psi q^{\dagger} \rangle \ . \tag{34}$$

By using the adjoint identity and the same operators H from Eqs. (30) and (32),

$$\langle \psi, H^{\dagger}\psi^{\dagger} \rangle = \langle \psi^{\dagger}, H\psi \rangle \ . \tag{35}$$

Equation (34) can be written as a function of the adjoint flux and the forward source distribution:

$$R = \langle \psi^{\dagger} q \rangle \ . \tag{36}$$

At this point, we know that the solution to the adjoint problem transports particles from the adjoint source (which is the detector or tally location) into the problem phase-space. The adjoint particles are scattered in energy and are transported in $-\Omega$ relative to the forward problem. However, it may not be immediately obvious how this adjoint solution relates to importance for the forward solution. Let us start with a simple illustrative example: a monoenergetic, monodirectional, point source. The forward source takes the form of a delta function:

$$q(\vec{r}, E, \widehat{\Omega}) = \delta(\vec{r} - \vec{r}_0)\delta(E - E_0)\delta(\widehat{\Omega} - \widehat{\Omega}_0) \ . \tag{37}$$

Using this definition of the forward source and evaluating Eq. (36), we obtain

$$\begin{aligned} R &= \langle \psi^{\dagger} q \rangle \\ &= \int_{V}\int_{E}\int_{\Omega} \psi^{\dagger}(\vec{r}, E, \widehat{\Omega}) q(\vec{r}, E, \widehat{\Omega}) d\widehat{\Omega} dE dV \\ &= \psi^{\dagger}(\vec{r}_0, E_0, \widehat{\Omega}_0) \ . \end{aligned} \tag{38}$$

This result shows that the solution to the adjoint equation is the detector response for the forward problem. As a result, the adjoint flux can be used as an indicator of a particle produced in $(\vec{r}, E, \widehat{\Omega})$ contributing to a response in the system. This indicator can be thought of as the particle's importance to achieving the tally or response objective. Consequently, it is often said that the adjoint is the importance function for the problem.

The adjoint solution is used in nuclear engineering for a number of applications, including reactor physics and perturbation theory.[14–17] However, Goertzel and Kalos' early work recognized its application for deep-penetration radiation shielding. Goertzel and Kalos[18] showed analytically that the exact adjoint solution, if used as an importance or weighting function for the forward Monte Carlo calculation, will result in a zero variance solution for the forward Monte Carlo problem. Further, Kalos[19] showed in a one-dimensional (1-D) infinite hydrogen slab problem that an analytically derived adjoint importance function significantly improved the speed to convergence for neutron transport in deep-penetration problems.

Goertzel and Kalos' finding that an exact adjoint can lead to a zero variance solution indicates that if a single particle is transported with the adjoint weighting function, its score will be the same as the total system response. Only a single particle is required to get an exact solution for the forward problem. This is prohibitive because obtaining an exact adjoint solution is just as computationally expensive as getting an exact forward solution. Instead, one seeks to obtain a good, but fairly inexpensive, estimate of the adjoint solution based on computational limitations. A good importance estimate should help reduce the variance in a reasonable amount of time and be relatively computationally inexpensive. A Monte Carlo solution can provide a continuous solution over the problem phase-space. However, as discussed in Sec. II.B, the

quality of this adjoint solution relies on the number of samples used to calculate it, and that may take a significant amount of time. A deterministic solution has the potential to offer equal or better solution confidence across the entire problem. However, it is discretized in space, energy, and angle. For deep-penetration importance functions, we opt for deterministically obtained solutions due to the solution's equally distributed validity.

III.B.2. Implementation

Coveyou et al.[20] expanded on Goertzel and Kalos' work by interpreting in which ways the adjoint solution could be adapted for Monte Carlo VR. In particular, they investigated the choice of biasing schemes and how effective they were at VR for a simple 1-D problem. They reiterated that the adjoint solution is a good estimate for importance but should not be calculated explicitly and rather should be estimated by a simpler model. The adjoint function is not necessarily the most optimal importance function; however, it is likely the closest and most obtainable estimate of importance that can be calculated.[20] They concluded that source biasing by the solution to the adjoint equation or by the expected response is the best choice for Monte Carlo VR, as it can be used independently from any other VR technique and provides good results.

Tang and Hoffman[21] extended the work of Coveyou et al.[20] by generating VR parameters automatically for fuel cask dose rate analyses. In their work, Tang and Hoffman used the 1-D discrete ordinates code XSDRNPM-S (Ref. 22) to calculate the adjoint fluxes for their shielding problems. The results from this calculation were then used to generate biasing parameters for Monte Carlo; specifically, they aimed at generating parameters for energy biasing, source biasing, rouletting and splitting, and next-event estimation probabilities. They implemented their work in the SAS4 module in SCALE (Ref. 23); it was one of the earlier implementations of a fully automated deterministic biasing procedure for Monte Carlo.

III.C. The Contributon Solution for Importance

Contributon theory is another useful concept that can be used as a measure of importance.[24–26] However, contributon theory quantifies importance differently from adjoint theory. In contributon transport, a pseudo particle, i.e., the contributon, is defined. The contributon carries response in the problem system from the radiation source to a detector. The total number of contributons in a system are conserved by the contributon conservation principle: All contributons that are emitted from the source eventually arrive at the detector. Much of the work in this realm has been done by Williams,[24] Williams and Manohara,[25] and Williams.[26]

The contributon transport equation can be derived in a form analogous to the forward [Eq. (29)] and adjoint [Eq. (31)] equations. The derivation of Eq. (40) and its corresponding variables are available in a number of the sources referenced in this section, so we will abstain from rederiving it here. The angular contributon flux is defined as the product of the forward and adjoint angular fluxes:

$$\Psi(\vec{r}, E, \hat{\Omega}) = \psi^{\dagger}(\vec{r}, E, \hat{\Omega})\psi(\vec{r}, E, \hat{\Omega}) \ . \tag{39}$$

The contributon transport equation is

$$\hat{\Omega} \cdot \nabla\Psi(\vec{r}, E, \hat{\Omega}) + \widetilde{\Sigma}_t(\vec{r}, E, \hat{\Omega})\Psi(\vec{r}, E, \hat{\Omega}) = \int_{4\pi}\int_0^{\infty} \widetilde{p}(\vec{r}, \hat{\Omega}' \rightarrow \hat{\Omega}, E' \rightarrow E)\widetilde{P}(\vec{r}, \hat{\Omega}', E') \times \widetilde{\Sigma}_t(\vec{r}, E', \hat{\Omega}')\Psi(\vec{r}, E', \hat{\Omega}')dE'\,d\hat{\Omega}' + \widehat{p}(\vec{r}, E, \hat{\Omega})R \ . \tag{40}$$

The units of phase-space are the same as those in the forward and adjoint transport equations. The symbols decorated with tildes denote variables that are unique to the contributon equation; $\widetilde{p}$ and $\widetilde{P}$ are both probability functions related to scattering, and $\widetilde{\Sigma}$ are effective cross sections. The effective cross sections are given by

$$\widetilde{\Sigma}_t(\vec{r}, E, \hat{\Omega}) = \widetilde{\Sigma}_s(\vec{r}, E, \hat{\Omega}) + \widetilde{\Sigma}_a(\vec{r}, E, \hat{\Omega}) = \frac{\int\int \Sigma_s(\vec{r}, \hat{\Omega}'' \cdot \hat{\Omega}, E \rightarrow E'')\psi^{\dagger}(\vec{r}, \Omega'', E'')d\Omega''dE''}{\psi^{\dagger}(\vec{r}, E, \hat{\Omega})} + \frac{Q^{\dagger}(\vec{r}, E, \hat{\Omega})}{\psi^{\dagger}(\vec{r}, E, \hat{\Omega})} \ . \tag{41}$$

Note here that the effective scattering and absorption cross sections are adjoint flux dependent. Where the adjoint flux becomes small, the interaction probabilities will become large. As a result, in regions where the adjoint flux is high, interaction probabilities become low, causing fewer interactions and more streaming. Conversely, regions with low adjoint fluxes, like the problem boundary, will have a very high cross section, thus encouraging particle transport back toward the adjoint source. This increased probability of interaction in low-flux regions encourages response particle (contributon) transport toward the detector or tally, thus contributing to a response.

The scattering probability of a contributon at position $\vec{r}$, E', and $\widehat{\Omega}'$ is

$$\widetilde{P}(\vec{r},\widehat{\Omega}',E') = \frac{\widetilde{\Sigma}_s(\vec{r},E',\widehat{\Omega}')}{\widetilde{\Sigma}_t(\vec{r},E',\widehat{\Omega}')} \ , \tag{42}$$

and the probability that a contributon scattering at $\vec{r}$, E', and $\widehat{\Omega}'$ will scatter into $d\widehat{\Omega}\,dE$ is

$$\widetilde{p}(\vec{r},\widehat{\Omega}' \rightarrow \widehat{\Omega}, E' \rightarrow E) = \frac{\Sigma_s(\vec{r},\widehat{\Omega}'\cdot\widehat{\Omega}, E' \rightarrow E)\psi^{\dagger}(\vec{r},E,\widehat{\Omega})}{\iint\Sigma_s(\vec{r},\widehat{\Omega}'\cdot\widehat{\Omega}'', E' \rightarrow E'')\psi^{\dagger}(\vec{r},E'',\widehat{\Omega}'')d\widehat{\Omega}''dE''} \ . \tag{43}$$

The distribution function governing the contributon source is

$$\widehat{p}(\vec{r},E,\widehat{\Omega}) = \frac{\psi^{\dagger}(\vec{r},E,\widehat{\Omega})Q(\vec{r},E,\widehat{\Omega})}{\iiint\psi^{\dagger}(\vec{r}',E',\widehat{\Omega}')Q(\vec{r}',E',\widehat{\Omega}')d\widehat{\Omega}'dE'dV'} \ . \tag{44}$$

Note that the contributon source is actually defined in Eq. (40) by the product of $\widehat{p}$ and R, where R is the contributon production rate and is given by the integral of the adjoint flux and the forward source:

$$\begin{aligned} R &= \iiint\psi^{\dagger}(\vec{r},E,\widehat{\Omega})Q(\vec{r},E,\widehat{\Omega})d\widehat{\Omega}dEdV \\ &= \langle\psi^{\dagger}Q\rangle, \end{aligned} \tag{45}$$

which is recognizable as the system response described in Sec. III.B. By integrating Eq. (40) over all phase-space and ensuring that the function $\widehat{p}$ is normalized, it can also be shown that

$$R = \langle\widetilde{\Sigma}_a\Psi\rangle \ , \tag{46}$$

or the rate at which contributons die in the detector is the same as the rate at which they are produced by the contributon source.

Knowing that R is the contributon production rate, let us consider the probability that a particle will be absorbed in the detector, or P, given by

$$P = \langle\Sigma_a\psi\rangle \ . \tag{47}$$

Adding a factor of $\psi^{\dagger}/\psi^{\dagger}$ to the terms on the right side, this becomes

$$P = \left\langle\frac{\Sigma_a}{\psi^{\dagger}}\psi\psi^{\dagger}\right\rangle \ . \tag{48}$$

By using the identities from the contributon equation, this is also

$$P = \langle\widetilde{\Sigma}_a\Psi\rangle \ . \tag{49}$$

Next, substituting the definition from Eq. (46) into Eq. (49), it follows that

$$P = R \ . \tag{50}$$

This is the same contributon conservation principle introduced at the beginning of this section. Williams noted that one could go so far as to transport contributons rather than real particles with Monte Carlo. Because every particle transported would eventually reach the detector and give an exact value for R [as shown by Eq. (50)], this would lead to a zero variance solution. However, the nature of solving the contributon equation with Monte Carlo (or any other transport mechanism) involves knowing the exact solution to the adjoint equation and so relies on the same computational obstacles as solving the adjoint transport equation.

As mentioned in Sec. III.B the adjoint flux is an indicator of a particle's importance to inducing a response. Conversely, the contributon flux describes the importance of a particle to the solution. Becker's thesis[27] aptly points out that this is illustrated most dramatically in a source-detector problem, where the forward source has little importance to the adjoint source but does have importance to the problem solution. As a result, both the contributon solution and the adjoint

solution can be considered importance functions for a problem, but the importance that they describe differs.

Williams recognized the applications of contributons to shield design and optimization in an extension of contributon theory called spatial channel theory. In particular, Williams noted that variables relevant to contributon response were useful in determining transport paths through media.[26,28] A study of different contributon values throughout the system could enlighten users on regions with higher response potential. This could then be used to intelligently choose regions for detector locations or add to shielding. The contributon values in this theory include the contributon flux, the contributon density, the contributon current, or the contributon velocity.[29] In this way, the user could find the particles most influential to the response of the system. A region with high response potential is the most important to a detector tally. The variables of response described by Williams are the response potential, the response current, and the response vorticity.[25]

Contributon theory and spatial channel theory have been applied successfully to shielding analyses[28,30] due to their ability to show particle flow between a source and response effectively. Williams and Engle showed that spatial channel theory can be used in reactor shielding analyses. In their work, they used contributon currents to determine preferential flow paths through the Fast Flux Test Facility.[28] Seydaliev and Henderson[30] used angle-dependent forward and adjoint fluxes and currents to visualize the contributon flux for simple source-detector problems. In this work, they showed that contributon flow in the system behaves much like a fluid between the source and detector, following preferential flow paths more densely. Seydaliev and Henderson also observed ray effects in the contributon flux for high-energy photons, and traditional methods like using a first collision source did not remedy the issue. The contributon formulation of particle transport can show important particle flow paths between a source and a detector, but it is still not immune to computational obstacles that exist for standard forward and adjoint transport.

Sections III.A through III.C have described various ways to define and quantify importance for a problem. As discussed in Sec. III.A, generating an importance function with Monte Carlo is limited in that the quality of the importance map is only as good as the regions that are sampled. For deep-penetration problems, it may be prohibitively difficult to obtain adequate importance sampling with traditional Monte Carlo methods.

Deterministically obtained importance functions, however, offer the benefit of a solution that is equally valid across all of the problem solution space. This is because the deterministic solution's precision is limited by convergence criteria, not sampling of individual particles. Using a deterministic solution is often faster and much less computationally intensive than Monte Carlo for importance quantification. As a result, many hybrid methods opt to use deterministically obtained importance functions to generate VR parameters for Monte Carlo transport.

IV. AUTOMATED VR METHODS FOR LOCAL SOLUTIONS

Sections IV, V, and VI describe different ways that deterministically obtained importance functions can be applied to VR methods in practice. Local VR methods are those that optimize a tally response in a localized region of the problem phase-space. These types of problems may be the most immediately physically intuitive to a user, where a person standing x meters away from a source may wish to know his or her personal dose rate. In this section, notable automated deterministically driven VR methods that have been designed for such localized response optimization are described. Recall that Booth's importance generator (Sec. II.C) was also designed for localized tally results, but it will not be elaborated upon here.

IV.A. CADIS METHOD

In 1997, Wagner and Haghighat[31] introduced the CADIS method[32,33] as a tool for automatic VR for local tallies in Monte Carlo. CADIS was unique in that it used the adjoint solution from a deterministic simulation to consistently bias the particle distribution and particle weights. Earlier methods had not ensured the consistency between source biasing and particle birth weights. CADIS was applied to a large number of application problems and performed well in reducing the variance for local tallies.[34]

The next several paragraphs present and discuss the theory supporting CADIS. Note that the theory presented is specific to space-energy CADIS, which is what is currently implemented in existing software. The original CADIS equations are based on space and energy $(\vec{r}, E)$ dependence, but not angle, so $\phi^\dagger$ can be used rather than $\psi^\dagger$. This does not mean that CADIS is not applicable to angle. This is merely a choice made by the software and method developers given the computational resources required to calculate and store full angular flux data sets

and the inefficiency that using angular fluxes might pose for problems where angle dependence is not paramount.

In trying to reduce the variance for a local tally, we aim to encourage particle movement toward the tally or detector location. In other words, we seek to encourage particles to induce a detector response while discouraging them from moving through unimportant regions in the problem. Recall from Eqs. (34) and (36) that the total system response can be expressed as either an integral of $\psi^\dagger q_e$ (the adjoint flux and the forward source) or $\psi q_e^\dagger$ (the forward flux and the adjoint source). Also, recall that the adjoint solution is a measure for response importance.

To generate the biased source distribution for the Monte Carlo calculation, $\widehat{q}$ should be related to its contribution to inducing a response in the tally or detector. It follows, then, that the biased source distribution is the ratio of the contribution of a cell to a tally response to the tally response induced from the entire problem. Thus, the biased source distribution for CADIS is a function of the adjoint scalar flux and the forward source distribution q in region $(\vec{r}, E)$ and the total response R:

$$\widehat{q} = \frac{\phi^\dagger(\vec{r}, E) q(\vec{r}, E)}{\iint \phi^\dagger(\vec{r}, E) q(\vec{r}, E) dE d\vec{r}} = \frac{\phi^\dagger(\vec{r}, E) q(\vec{r}, E)}{R} . \tag{51a}$$

The starting weights of the particles sampled from the biased source distribution $\widehat{q}$ must be adjusted to account for the biased source distribution. As a result, the starting weights are a function of the biased source distribution and the original forward source distribution:

$$w_0 = \frac{q}{\widehat{q}} = \frac{R}{\phi^\dagger(\vec{r}, E)} . \tag{51b}$$

Note that when Eq. (51a) is placed into Eq. (51b), the starting weight is a function of the total problem response and the adjoint scalar flux in $\vec{r}, E$. The target weights for the biased particles are given by

$$\widehat{w} = \frac{R}{\phi^\dagger(\vec{r}, E)} , \tag{51c}$$

where the target weight $\widehat{w}$ is also a function of the total response and the adjoint scalar flux in region $\vec{r}, E$. The equations for $\widehat{w}$ and w_0 match; particles are born at the same weight of the region into which they are born. Consequently, the problem limits excessive splitting and rouletting at the particle births in addition to consistently biasing the particle source distribution and weights. This is the "consistent" feature of the CADIS method.

CADIS supports adjoint theory by showing that using the adjoint solution $\phi^\dagger$ for VR parameter generation successfully improves Monte Carlo calculation run time. CADIS showed improvements in the FOM when compared to analog Monte Carlo on the order of 10^2 to 10^3 and on the order of five when compared to "expert" determined or automatically generated weight windows[32,35] for simple shielding problems. For more complex shielding problems, improvements in the FOM were on the order of 10^1 (Refs. 31 and 32). Note that CADIS improvement is dependent on the nature of the problem and that these are merely illustrative examples.

IV.B. Becker's Local Weight Windows

Becker's work in the early 2000s also explored generating biasing parameters for local source-detector problems.[27] Becker noted that in traditional weight window–generating methods, some estimation of the adjoint flux is used to bias a forward Monte Carlo calculation. The product of this weight window biasing and the forward Monte Carlo transport ultimately distributed particles in the problem similarly to the contributon flux. In his work, Becker used a formulation of the contributon flux, as described in Eq. (39), to optimize the flux at the forward detector location. The relevant equations are given by Eqs. (52a) through (52f).

First, the scalar contributon flux ϕ^c, which is a function of space and energy, is calculated with a product of the deterministically calculated forward and adjoint fluxes, where

$$\phi^c(\vec{r}, E) = \phi(\vec{r}, E)\phi^\dagger(\vec{r}, E) . \tag{52a}$$

This is then integrated over all energy to obtain a spatially dependent contributon flux

$$\widetilde{\phi}^c(\vec{r}) = C_{norm} \int_0^\infty \phi^c(\vec{r}, E) dE , \tag{52b}$$

where the normalization constant C_{norm} for a given detector volume V_D is

$$C_{norm} = \frac{V_D}{\int_{V_D}\int_0^\infty \phi^c(\vec{r},E)dEdV} \quad . \tag{52c}$$

The space- and energy-dependent weight windows are given by

$$\overline{w}(\vec{r},E) = \frac{B(\vec{r})}{\phi^\dagger(\vec{r},E)} \quad , \tag{52d}$$

where

$$B(\vec{r}) = \alpha(\vec{r})\widetilde{\phi}^c(\vec{r}) + 1 - \alpha(\vec{r}) \tag{52e}$$

and

$$\alpha(\vec{r}) = \left[1 + \exp\left(\frac{\widetilde{\phi}^c_{\max}}{\widetilde{\phi}^c(\vec{r})} - \frac{\widetilde{\phi}^c(\vec{r})}{\widetilde{\phi}^c_{\max}}\right)\right]^{-1} \quad . \tag{52f}$$

Becker found that this methodology compared similarly to CADIS for local solution VR for a large challenge problem comprising nested cubes. The particle density throughout the problem was similar between CADIS and Becker's local weight window. The FOMs were also relatively similar but were reported only with Monte Carlo calculation run times (meaning that the deterministic run times were excluded). Note that Becker's method requires both a forward and an adjoint calculation to calculate the contributon fluxes while CADIS requires only an adjoint calculation.

V. AUTOMATED VR METHODS FOR GLOBAL SOLUTIONS

Variance reduction methods for global solutions are designed to obtain an even distribution of error across several tallies or a tally map that spans the entire problem phase-space. Section IV details several methods that automate VR for localized tallies. However, for global solutions these methods do not work well. The global tally suffers from a large range in variance across the physical problem space, and the solution is dependent on the flux distribution throughout the problem.

This section describes several methods that provide automated VR for global solutions or multiple tallies. The general principle that these methods follow is that by distributing particles evenly throughout the Monte Carlo problem, a global tally will have approximately the same sample size in each region, resulting in a uniform variance across the tally. This often requires a forward deterministic solution to determine the density of forward particles throughout the problem and subsequently using that forward distribution to aid in generating an importance map. This section summarizes the theory behind a number of existing global VR methods. The section concludes with a summary of how the methods performed and in which problems they performed well.

V.A. Cooper's Isotropic Weight Windows

Cooper and Larsen developed a weight window technique to reduce the variance of Monte Carlo global solutions[36] using a calculation of the forward flux from solutions obtained from diffusion, quasi diffusion,[37] or pure Monte Carlo. In their work, Cooper and Larsen utilized a forward solution to the transport equation to generate weight window values to uniformly distribute particles throughout the problem. By doing so, the variance in the scalar flux remained relatively constant throughout the problem for a problem-wide tally rather than rising significantly with increasing distance from the forward source. Cooper's "isotropic" weight windows (named because they were not dependent on $\widehat{\Omega}$) dependent on $\vec{r}$ are given by

$$\overline{ww}(\vec{r}) = \frac{\phi(\vec{r})}{\max\phi(\vec{r})} \quad , \tag{53a}$$

$$ww(\vec{r})_{top} = \rho\overline{ww}(\vec{r}) \quad , \tag{53b}$$

and

$$ww(\vec{r})_{bottom} = \frac{\overline{ww}(\vec{r})}{\rho} \quad , \tag{53c}$$

where ρ is the weight window scaling factor. Note that by setting the weight window target value to be inversely proportional to the total flux in the cell, the density of particles throughout the problem becomes roughly constant. Also note from Eq. (53a) that the weight windows depend on space only.

In practice, Cooper's algorithm iteratively switches between solving the diffusion equation with transport correctors (Eddington factors described by Ref. 38) and Monte Carlo solutions; this process is known as quasi diffusion.[37,38] An initial quasi-diffusion solution is used to generate weight windows, and then after a relatively short run time, the Monte Carlo solution is used to

generate updated Eddington factors for the quasi-diffusion solution.

Because Cooper's method depends on Monte Carlo to generate the Eddington factors for the quasi-diffusion problem, this method is limited by the iterative switch between the quasi-diffusion solution and the Monte Carlo solution. The frequency with which this switching happens is entirely up to the user but may drastically affect the efficiency of the method. Further, Cooper notes that we do not know at what point in time (for which number of N particles) the Monte Carlo solution becomes more accurate than the quasi-diffusion solution, which is an important issue in choosing solution parameters.

V.B. Becker's Global Weight Windows

Becker, in addition to developing the local VR method discussed in Sec. IV.B, developed a global space-energy weight correction method both with (Sec. VI) and without directional biasing.[27,39] Becker's global method uses a formulation of the space-dependent contributon flux, as with the local weight windows described in Sec. IV.B. For reference, those are defined in Eqs. (52a) and (52b).

Becker defines the spatially dependent contributon flux parameter as $B(\vec{r})$, where

$$B(\vec{r}) = \widetilde{\phi}^{c}(\vec{r}) \ . \tag{54}$$

Becker's method defines a different adjoint source distribution depending on the response desired for the calculation. To optimize the flux the adjoint source is defined as

$$q^{\dagger}(\vec{r},E) = \frac{1}{\phi(\vec{r},E)} \ . \tag{55a}$$

If the detector response is desired, then

$$q^{\dagger}(\vec{r},E) = \frac{\Sigma_d(\vec{r},E)}{\int_0^{\infty} \phi(\vec{r},E)\Sigma_d(\vec{r},E)dE} \tag{55b}$$

can be used instead. The space- and energy-dependent weight windows are then a function of the contributon flux, where

$$\overline{w}(\vec{r},E) = \frac{B(\vec{r})}{\phi^{\dagger}(\vec{r},E)} \ . \tag{56}$$

The process followed by Becker's global method uses two deterministic calculations to generate weight windows for the Monte Carlo calculation. First, the forward flux is calculated deterministically and used to construct the adjoint source distribution. After the adjoint solution has been obtained, the contributon flux is calculated. The contributon flux and the adjoint flux are then used to construct the weight windows.

Becker's method aims to distribute response evenly throughout the problem. However, like FW-CADIS (discussed in Sec. V.C), the global response weight windows are proportional to the forward response,

$$\overline{w}(\vec{r},E) \propto \frac{\int \Sigma(\vec{r},E)\phi(\vec{r},E)dE}{\Sigma(\vec{r},E)} \ , \tag{57}$$

rather than the forward flux as in Cooper's method, where $\overline{w}(\vec{r},E) \propto \phi(\vec{r},E)$.

In implementation, both Becker's and Cooper's global methods undersampled the source (in comparison to FW-CADIS, which is described in Sec. V.C) for a specified calculation time. However, Becker's method sampled approximately one-third the number of particles that Cooper's method did. Notably, Becker's method did obtain better relative uncertainties for low-flux regions in the problem.

V.C. FW-CADIS

In 2007, Peplow et al.[40] proposed three methods by which VR could be decreased in global mesh tallies in deep-penetration radiation transport problems. The first method, using a CADIS calculation where the adjoint source is defined at the problem boundary, aimed at moving particles outward to the problem edges. The second method used standard CADIS but instead defined each cell as equally important, so the adjoint source was defined equally throughout the problem phase-space. The last method, FW-CADIS, distributed the adjoint source across mesh cells as an inverse relation to the forward response of the cell. In their work, Peplow et al. found that the first method had large uncertainties in areas of the problem far from the boundary; the second method performed slightly, but not significantly, better than analog; and the third method had the most uniform uncertainty distribution.

FW-CADIS (Refs. 41, 42, and 43) extended the work by Cooper and the CADIS method. Like Becker's method, FW-CADIS uses a forward deterministic calculation to determine the source distribution for the adjoint

calculation. Unlike Becker's method, which used contributon fluxes to construct weight windows, the CADIS method uses adjoint fluxes as the basis of the weight window values. Similar to Cooper's method, however, FW-CADIS uses the forward calculation to determine how to evenly distribute particles throughout the problem. Like CADIS, FW-CADIS uses the adjoint solution from the deterministic calculation to generate consistent source biasing, weight windows, and particle birth weights.

The adjoint source for the adjoint calculation is dependent on the desired response for the system. The generic description for the adjoint source is given by Eq. (58), and more specific parameters are given by Eqs. (59a), (59b), and (59c). First, we can describe a general form of the adjoint source definition for all phase-space P as

$$q^{\dagger}(P) = \frac{\Sigma_d(P)}{R} \quad . \tag{58}$$

Thus, the adjoint source is dependent on the detector (or tally) cross section and whatever response is being calculated in the system. Depending on whether the response is a flux or a dose rate, the adjoint source will differ. For example, the adjoint source for the spatially dependent global dose $\int \phi(\vec{r},E)\Sigma_d(\vec{r},E)dE$ is

$$q^{\dagger}(\vec{r},E) = \frac{\Sigma_d(\vec{r},E)}{\int \Sigma_d(\vec{r},E)\phi(\vec{r},E)dE} \quad . \tag{59a}$$

The adjoint source for the spatially dependent total flux $\int \phi(\vec{r},E)dE$ is

$$q^{\dagger}(\vec{r}) = \frac{1}{\int \phi(\vec{r},E)dE} \quad . \tag{59b}$$

Last, the adjoint source for the energy-dependent and spatially dependent flux $\phi(\vec{r},E)$ is

$$q^{\dagger}(\vec{r},E) = \frac{1}{\phi(\vec{r},E)} \quad . \tag{59c}$$

The process followed by FW-CADIS is to initially run a deterministic forward calculation to obtain the forward response. This solution is used to create the source distribution for the adjoint problem. A second deterministic calculation is run to obtain the adjoint solution. The adjoint solution is then used to generate VR parameters in the same manner as CADIS.

V.D. Other Notable Methods

Baker and Larsen showed that the exponential transform can be used to generate VR parameters for global low-variance solutions in Monte Carlo.[44] In this work, Baker and Larsen used a forward diffusion solution to generate parameters for a combination of VR techniques: implicit capture and weight cutoff, geometry splitting/rouletting with implicit capture and weight cutoff, and the exponential transform combined with implicit capture and a weight cutoff. The exponential transform method was then compared to the other combinations of VR techniques to quantify its success. In their work, Baker and Larsen found that the exponential transform approach did not work well for highly scattering problems, where geometry splitting and rouletting were generally better options. Their work did not focus on generating weight window values nor was it tested on deep-penetration shielding problems.

While the aforementioned methods in this and Secs. V.A through V.C use deterministically obtained solutions to generate importance maps, it should be noted that not all methods use this approach. Booth's and Hendricks' methods used initial Monte Carlo calculations to reduce the relative error in tallies. Two methods in the global VR realm are notable in that they too use Monte Carlo estimates of the flux to generate VR parameters.[45,46] Van Wijk et al.[45] developed an automated WWG that used a Monte Carlo calculation of the forward flux to generate weight window values. The weight window target values could be determined based on either a flux-centered scheme like Cooper's [Eq. (53a)] or by using a ratio of the square roots of the fluxes. The second method is a combination of Cooper's weight window target values and knowing that the relative error in a region is proportional to the square root of the number of particles. Van Wijk et al. applied their methods to a pressurized water reactor facility and observed a FOM increase by a factor of >200 when compared to analog Monte Carlo. However, as with other Monte Carlo–generated VR parameters, for deep-penetration problems this approach relies on adequate sampling of all phase-space, which could be computationally prohibitive.

The Method of Automatic Generation of Importances by Calculation (MAGIC) method was proposed in parallel by Davis and Turner.[46] As with Van Wijk et al.'s method, the MAGIC method uses an analog forward

Monte Carlo—potentially with several iterations—calculation to generate weight windows. The initial Monte Carlo runs used to generate the importance map took less time to converge by using multigroup (rather than continuous energy) cross-section data as well as energy cutoffs. MAGIC converged on a finalized importance map by iteratively running several lower-fidelity Monte Carlo calculations.

Davis and Turner[46] compared three variants of MAGIC to FW-CADIS in ITER fusion energy systems. These three variants used different weight window adjustments for importances: weight windows in mesh cells based on existing weight information, weight windows in mesh cells based on flux information, and weight windows in mesh cells based on population density. It was concluded that the most effective method for VR of those proposed in the paper was MAGIC's weight window in mesh cells based on flux information. In this case, FW-CADIS's FOM was 65% that of MAGIC's. This compared similarly to Van Wijk et al.'s method, where the flux-based results continued improving the FOM as the computational time increased. Davis and Turner did not make it clear how many iterations were required, on average, to generate the finalized weight window map or if the time to iteratively generate the importance map was included in the FOM. While FW-CADIS's FOM was lower than MAGIC's, FW-CADIS had the highest fraction of cell voxels with very low relative errors.

Peplow[47] compared the performance of Cooper's method, Van Wijk et al.'s method, Becker's method, and FW-CADIS across a number of shielding calculations. For a simple shielding problem, FW-CADIS had the shortest run time, which included the forward and adjoint deterministic run times, and had a FOM 80 times higher than the analog calculation and more than three times higher than the next best hybrid method. Van Wijk et al.'s method was the only method other than FW-CADIS to pass all statistical convergence checks for the problem, but its reported FOM was lower than either Becker's method or FW-CADIS. In a second deep-penetration shielding problem, FW-CADIS was the only method that passed all statistical convergence checks. FW-CADIS also had the highest reported FOM for this problem. For all of the methods, the timing was comparable. Peplow also ran two "challenge" problems. As with the first two problems, FW-CADIS outperformed the other methods and passed all statistical checks. Becker's method was consistently comparable to FW-CADIS in reported FOMs but passed all of the statistical checks only in a single challenge problem. Becker's method also performed relatively better than the other methods in deep-penetration challenge problems.

The ubiquity and continued development of global VR methods illustrate the need and desire for them in the nuclear engineering community. Some of the methods discussed in this section, including Becker's global weight windows, Cooper's weight windows, Van Wijk et al.'s method, and FW-CADIS, have been applied to large application problems and compared to other methods. When compared to analog Monte Carlo, all of the methods reduce the time to a good solution, thus improving the final FOM. When compared against one another, FW-CADIS consistently outperforms the other methods.

VI. AUTOMATED ANGLE-INFORMED VR METHODS

In a number of problems, the angular dependence of the flux is significant enough that biasing in space and energy exclusively is not sufficient. As a result, a subset of hybrid methods was developed to incorporate some degree of the flux anisotropy in VR parameters. Without explicitly calculating the angular flux, which is memory and storage intensive, methods attempted to approximate the angular flux using other information more readily accessible to them. These approaches are broadly categorized as methods that bias using population control methods (such as weight windows) and methods that bias with modified sampling methods (such as the exponential transform). Initial approaches to angular biasing focused on approximating the angular flux ψ as a separable function of the scalar flux and an angle-dependent multiplier. These approximations of the flux were then used to generate biasing parameters dependent on angle for highly angular-dependent problems. In this section, methods that generate VR parameters dependent on angle or that include angular information are described.

VI.A. Angular Biasing with Population Control Methods

VI.A.1. AVATAR

The Automatic Variance and Time of Analysis Reduction[12,48] (AVATAR) method generates three-dimensional space-, energy- and angle-dependent weight windows for Monte Carlo. The implementation of AVATAR by Van Riper et al.[12,48] uses a relatively coarse-mesh and few-angle deterministic calculation in THREEDANT (Ref. 49), approximating the angular flux as a function of the scalar flux, and then subsequently passes those flux values through a postprocessing code, Justine, to generate weight windows for MCNP (Ref. 2). The AVATAR approach to

determining the angular flux uses an approximation of the angular flux based on the maximum entropy distribution, which is briefly summarized in the next few paragraphs.

VI.A.I.a. Information Theory

First, for a given set of discrete values x_i, $i = 1, 2, \cdots n$, that are passed to a function $f(x)$, the expectation value of that function is given by

$$\langle f(x)\rangle = \sum_{i=1}^{n} p_i f(x_i) \ . \tag{60}$$

For the probability distribution $p_i = p(x_i)$, $i = 1, 2, \cdots n$, the entropy of p is defined as

$$H(p) = -K \sum_i p_i \ln p_i \ , \tag{61}$$

where K is a positive constant. A proof that this is indeed the associated maximal entropy associated with all p_i is given in Ref. 50. For a continuous probability density function $p(x)$ over the interval I, the entropy of the continuous function is

$$H(p) = -K \int_I p(x) \ln p(x) dx \ . \tag{62}$$

To maximize either of these distributions, while also maintaining that $\sum p_i = 1$, one can use Lagrangian multipliers λ and μ:

$$p_i = e^{-\lambda - \mu f(x_i)} \ . \tag{63}$$

This set of equations can be solved using

$$\langle f(x)\rangle = -\frac{\partial}{\partial \mu} \ln Z(\mu) \tag{64a}$$

and

$$\lambda = \ln[Z(\mu)] \ , \tag{64b}$$

where

$$Z(\mu) = \sum_i e^{-\mu f(x_i)} \ . \tag{64c}$$

Jaynes[50,51] showed that the maximum entropy probability distribution function corresponding to Eqs. 61 though 64 is given by

$$p_i = \exp\left[-(\lambda_0 + \lambda_1 f_1(x_1) + \cdots + \lambda_m f_m(x_i))\right] \ , \tag{65}$$

and the entropy of this distribution is given by

$$S_{\max} = \lambda_0 + \lambda_1 \langle f_1(x)\rangle + \cdots + \lambda_m \langle f_m(x)\rangle \ . \tag{66}$$

In this case, the constant K from Eq. (61) has been set to 1.

The maximum entropy approach to calculating a probability distribution function is an attractive option given limited information about that distribution. This method's power lies in that it deduces a function given limited information but does not place too great of an importance on missing or unwarranted information. Furthermore, a distribution ascertained from this methodology will encompass all distributions with smaller entropies that satisfy the same constraints. Thus, the method provides the most widely applicable probability distribution function for the system that has been defined.

Moskalev showed that by using the maximum entropy approach, a distribution function could be reconstructed from a (truncated) Legendre expansion.[52] This is particularly applicable to radiation transport because scattering terms are often truncated Legendre expansions. In his application, Moskalev derived a generalized form of reconstructing a probability distribution from a truncated expansion, where the true function represented by a Legendre polynomial series,

$$f(L, \mu) = \sum_{l=0}^{L} -\frac{2l+1}{2} f_l P_l(\mu) \ , \tag{67}$$

could be associated with an adjusted function (obtained from maximizing the entropy of the known values),

$$\widetilde{f}(L, \mu) = \exp\left(\sum_{l=0}^{L} \lambda_l P_l(\mu)\right) \ , \tag{68}$$

such that

$$(f, P_l) = (\widetilde{f}, P_l); \quad l = 0, \cdots, L \ , \tag{69}$$

where λ_l are the Lagrange multipliers; $\widetilde{f}$ and f lie within a positive set of functions ($\in \Phi$) and are assumed to be a function of μ such that $f(\mu) \geq 0, \mu \in [-1, 1]$; and (,) is the inner product. These generalized equations were then applied to group-to-group scattering probability distribution functions, as well as reconstructing a $L = 3$ function. The reconstruction showed agreement except near the extrema of μ.

Walters and Wareing[53,54] showed that the angle-dependent source definition for a discrete ordinates transport problem could be calculated using Moskalev's approach.[52] In their method, Walters and Wareing used this approach to reconstruct the source distribution of particles in each cell from the source moments. For standard methods, the source in a cell expanded in Legendre moments is

$$S_m(x) = S_{m,j}\left[P_0(x) + \frac{S^x_{m,j}}{S_{m,j}} P_1(x)\right] , \tag{70}$$

where

$S_{m,j}$ = average source in cell j, direction m

$S^x_{m,j} = P_1(x)$ moment of the source

P_0, P_1 = associated Legendre polynomials.

Using a normalized source distribution $s_m(x)$, where

$$S_m(x) = s_m(x) S_{m,j} , \tag{71}$$

the normalized distribution is

$$s_m(x) = [s_0 + s_1 P_1(x)] , \tag{72}$$

where s_0 and s_1 are the zeroth and first Legendre moments of the source, respectively. The source distribution derived from the maximum entropy distribution is

$$\widetilde{s}(x) = \frac{\lambda_{1,k}}{\sinh(\lambda_{1,j})} e^{\lambda_{1,j} P_1(x)} , \tag{73}$$

where $\widetilde{s}$ has normalized Legendre moments s_0 and s_1 that match $s_m(x)$. Because $\widetilde{s}$ satisfies the information that can be obtained about s_m, it can be used to reconstruct $S_m(x)$:

$$S_m(x) = \widetilde{s}_m(x) S_{m,j} . \tag{74}$$

The term $\lambda_{1,j}$ can be found with

$$s_1 = 3\left[\coth\left(\lambda_{1,j} - \frac{1}{\lambda_{1,j}}\right)\right] . \tag{75}$$

It should be noted that the same methodology that Walters and Wareing use to reconstruct the source distribution from the source moments can be used to reconstruct the angular flux in cells based on moments of the angular flux (i.e., the scalar flux and current).[53]

In their paper, Walters and Wareing[54] suggest that in place of solving Eq. (75) for $\lambda_{1,j}$, a rational polynomial can be used in its place to reduce computational time. The suggested polynomial for $0 \le \lambda_{1,j} \le 5$ is

$$\lambda_{1,j} = \frac{2.99821\left(\frac{s_{1,j}}{3}\right) - 2.2669248\left(\frac{s_{1,j}}{3}\right)^2}{1 - 0.769332\left(\frac{s_{1,j}}{3}\right) - 0.519928\left(\frac{s_{1,j}}{3}\right)^2 + 0.2691594\left(\frac{s_{1,j}}{3}\right)^3} , \tag{76}$$

and the suggested polynomial for for $\lambda \ge 5$ is

$$\lambda_{1,j} = \frac{1}{1 - \frac{s_{1,j}}{3}} . \tag{77}$$

A full derivation of Eq. (75) and how it satisfies the maximum entropy requirements can be found in Appendix A of Ref. 54.

In their application, Walters and Wareing found that this method was accurate over a fairly coarse mesh for the problems analyzed and the computed fluxes remained positive over the solution space. When compared to other methods, this approach performed much better on coarse meshes. However, the analysis was limited to 1-D problems. As mesh size grew finer, the method performed similarly to other methods. Near-vacuum boundary conditions, $\lambda_{1,j} \to \infty$ at the cell boundary, caused issues in calculating the flux in these cells.

VI.A.I.b. AVATAR Implementation

AVATAR uses a deterministically obtained solution of the adjoint scalar flux and adjoint currents to reconstruct the angular flux distribution. The angular flux distribution is then used to generate weight windows. AVATAR leveraged the methodology described by Walters and Wareing,[53,54] but instead of reconstructing the source distribution inside the cell, the maximum entropy method was used to reconstruct the angular fluxes. Thus, the angular flux ψ was reconstructed with the scalar flux ϕ and the current J.

AVATAR avoided generating explicit angular fluxes with THREEDANT (Ref. 49) by assuming that the adjoint angular flux is symmetric about the average adjoint current vector $J^\dagger$:

$$\psi^\dagger(\widehat{\Omega}) = \psi^\dagger(\widehat{\Omega} \cdot n) , \tag{78a}$$

where

$$n = \frac{J^\dagger}{\left\| J^\dagger \right\|} \ . \tag{78b}$$

Note that $n, J, \psi,$ and ϕ all have implied dependence on $(\vec{r}, E)$. The angular flux could then be reconstructed assuming that the angular flux is a product of the scalar flux and some angle-dependent function:

$$\psi^\dagger(\widehat{\Omega} \cdot n) = \phi^\dagger f(\widehat{\Omega} \cdot n) \ . \tag{78c}$$

Note that Eq. (78c) takes the form of Eq. (74). Thus, f is derived from the maximum entropy distribution:

$$f(\widehat{\Omega} \cdot n) = \frac{\lambda e^{(\widehat{\Omega} \cdot n)\lambda}}{2 \sinh \lambda} \ , \tag{78d}$$

and λ is a function of the average cosine $\overline{\mu}$:

$$\lambda = \frac{2.99821\overline{\mu} - 2.2669248\overline{\mu}^2}{1 - 0.769332\overline{\mu} - 0.519928\overline{\mu}^2 + 0.2691594\overline{\mu}^3} = \frac{1}{1 - \overline{\mu}} \tag{78e}$$

for $0 \leq \overline{\mu} < 0.8001$ and $0.8001 \leq \overline{\mu} < 1.0$, respectively. The variable $\overline{\mu}$ is defined as

$$\overline{\mu}(\vec{r}, E) = \frac{\left\| J^\dagger(\vec{r}, E) \right\|}{\phi^\dagger(\vec{r}, E)} \ . \tag{78f}$$

Equations (78e) and (78f) are exact in both isotropic and streaming conditions.[12]

Using the calculation of the angular flux described in Eqs. (78a) through (78f), angle-dependent weight windows can be constructed. AVATAR's space-, energy-, and angle-dependent weight window is given by

$$\overline{w}(\vec{r}, E, \widehat{\Omega}) = \frac{k}{\phi^\dagger(\vec{r}, E) f(\widehat{\Omega} \cdot n)} \ , \tag{79}$$

where k is a constant that can be adjusted to match the source distribution. In the case of AVATAR, k was used as a normalization factor to ensure that source particles are born with weights within the weight window. AVATAR exclusively generated weight windows and did not attempt to consistently bias the source distribution. Physically, the assumption behind AVATAR is that the adjoint angular flux is locally 1-D, so azimuthal symmetry is assumed.

VI.A.I.c. AVATAR Results

Van Riper et. al.[12,48] showed that AVATAR's angularly dependent weight windows improved the FOM (from five times to seven times) for a multiple-tally well-logging problem compared to the MCNP WWG. AVATAR was also compared to other methods in subsequent papers.[11] In an update of the MCNP WWG, AVATAR was compared to variants of the WWG and had a FOM of 79 while variants of the WWG had FOMs ranging from 105 to 119 (Ref. 11). However, the MCNP WWG required multiple iterations of Monte Carlo transport to converge on weight window values while AVATAR did not. Total run times for iteratively converging on weight window values were in the 200- to 300-min range, while AVATAR took roughly 5 min to converge on weight window values for the problem. Whether these calculations were performed in serial or parallel was not discussed.

The MCNP WWG has also been adapted to use weight window values seeded by a solution from AVATAR (Ref. 11). This method had FOMs comparable to the default MCNP WWG but required only one iteration to converge rather than three. This reduced the total transport run time from roughly 260 to 140 min but still required user experience and input to adequately set up and prepare the deterministic input for AVATAR.

The method used by AVATAR to produce angle-dependent weight windows successfully incorporated angular information into VR parameters for Monte Carlo with very little additional computational burden. However, because AVATAR was not fully automated, the user had to have knowledge on the use of the S_N deterministic solver in addition to the Monte Carlo methods they were trying to optimize. As a result, the user needed to adequately prepare the deterministic inputs, correctly specify the adjoint source for the deterministic solve, and then pass these values to postprocessing software.[11,55] The FOMs reported with AVATAR did not incorporate the additional time required for user setup and preparation of inputs. Though this is not a customary time inclusion, the burden of time for this process may be significant. Though more computationally efficient than the WWG, this aspect of AVATAR may be too substantive of an obstacle for new-user approachability. Further, it leaves more room for user-induced error.

The AVATAR method[12,48] used an approximation of the angular flux—without explicitly calculating it—to generate angle-dependent weight windows. It operated with the approximation that the angular flux was separable and symmetric about the average current

vector. The angular flux was then calculated using a product of a deterministically obtained scalar flux and an exponential function, derived from the maximum entropy distribution, that was a function of the scalar flux and the current. Space-, energy-, and angle-dependent weight windows for the Monte Carlo problem were then generated from the inverse of the angular flux. AVATAR improved the FOM for sample problems from two to five times but did not apply to problems where the flux was not azimuthally symmetric.

VI.A.2. Simple Angular CADIS

Simple Angular CADIS (Ref. 55) is built on the theory of CADIS and FW-CADIS but incorporates angular information in the methods without explicitly using angular flux solutions from the deterministic solution. Instead, the method reconstructs the angular flux in the same manner employed by AVATAR and additionally consistently biases the source distribution with the weight windows using the same methodology as CADIS and FW-CADIS. Recall that the original implementation of AVATAR did not have consistent source biasing. In their work, Peplow et al. implemented simple angular CADIS in MAVRIC, a hybrid methods software package distributed with the SCALE code base.[23] The Simple Angular CADIS method was implemented with two different approaches to VR: directionally dependent weight windows with directionally dependent source biasing and directionally dependent weight windows without directional source biasing.

VI.A.2.a Theory

The simple angular CADIS approach, like AVATAR, uses a reconstruction of the angular flux derived from the maximum entropy distribution (Sec. VI.A.1). In simple angular CADIS, the adjoint angular flux is approximated such that

$$\psi^{\dagger}(\vec{r},E,\widehat{\Omega}) \cong \phi^{\dagger}(\vec{r},E)\frac{1}{2\pi}f(\widehat{\Omega}\cdot\widehat{n}) \ , \tag{80}$$

where $f(\widehat{\Omega}\cdot\widehat{n})$ is given by the same Eqs. (78d), (78e), and (78f) as AVATAR. Note that this differs from AVATAR's reconstruction of the angular flux, Eq. (78a), by a factor of $1/2\pi$. As it was only dependent on μ, AVATAR's original approach assumed azimuthal symmetry but did not incorporate any factor of integration into the angular flux reconstruction. By including the azimuthal integration factor of $1/2\pi$, this version of $\psi^{\dagger}$ satisfies

$$\phi^{\dagger}(\vec{r},E) = \int \phi^{\dagger}\frac{1}{2\pi}f(\widehat{\Omega}\cdot\widehat{n})d\widehat{\Omega} \ . \tag{81}$$

The corresponding angle-dependent weight windows are then given by

$$\overline{w}(\vec{r},E,\widehat{\Omega}) = \frac{2\pi k}{\phi^{\dagger}(\vec{r},E)\,f(\widehat{\Omega}\cdot n)} \ . \tag{82}$$

For the version of simple angular CADIS with directionally dependent weight windows and without directional source biasing, the biasing parameters are given by Eqs. (83). The biased source distribution $\widehat{q}(\vec{r},E,\widehat{\Omega})$ is given by a combination of the standard CADIS biased source $\phi^{\dagger}(\vec{r},E)$ and the original directional source distribution $q(\widehat{\Omega}\cdot\widehat{d})$ such that

$$\begin{aligned}\widehat{q}(\vec{r},E,\widehat{\Omega}) &= \frac{1}{R}q(\vec{r},E)\phi^{\dagger}(\vec{r},E)\frac{1}{2\pi}q(\widehat{\Omega}\cdot\widehat{d}) \\ &= \widehat{q}(\vec{r},E)\frac{1}{2\pi}q(\widehat{\Omega}\cdot\widehat{d}) \ .\end{aligned} \tag{83a}$$

The direction $\widehat{d}$ is sampled using the original directional source distribution. The birth weight matches standard CADIS with

$$\begin{aligned}w_0(\vec{r},E,\widehat{\Omega}) &= \frac{q(\vec{r},E,\widehat{\Omega})}{\widehat{q}(\vec{r},E,\widehat{\Omega})} \\ &= \frac{R}{\phi^{+}(\vec{r},E)} \ ,\end{aligned} \tag{83b}$$

and the weight window target value is given by

$$\begin{aligned}\overline{w}(\vec{r},E,\widehat{\Omega}) &= \frac{R}{\phi^{\dagger}(\vec{r},E)}\frac{f(\widehat{\Omega}_0\cdot n(\vec{r}_0,E_0))}{f(\widehat{\Omega}\cdot n)} \\ &= \overline{w}(\vec{r},E)\frac{f(\widehat{\Omega}_0\cdot n(\vec{r}_0,E_0))}{f(\widehat{\Omega}\cdot n)} \ .\end{aligned} \tag{83c}$$

Note that the biased source distribution $\widehat{q}(\vec{r},E,\widehat{\Omega})$ is a function of the biased source distribution from standard space and energy CADIS and of the original directional source distribution. This is why this method has directional weight windows but not directional source biasing.

For the version of simple angular CADIS with directionally dependent weight windows and with directional

source biasing, the biasing parameters are given by the equations summarized in Eqs. (84). The biased source distribution is given by a combination of the space-energy biased source distribution, the original directional source distribution, and a directionally dependent biased source distribution $f(\widehat{\Omega}\cdot\widehat{n}_0)$ such that

$$\begin{aligned}\widehat{q}(\vec{r},E,\widehat{\Omega}) &= \frac{1}{Rc}q(\vec{r},E,\widehat{\Omega})\phi^{\dagger}(\vec{r},E,\widehat{\Omega})\\ &= \left[\frac{1}{R}q(\vec{r},E)\phi^{\dagger}(\vec{r},E)\right]\\ &\times\ \left[\frac{1}{c}\frac{1}{2\pi}q(\widehat{\Omega}\cdot\widehat{d})\frac{1}{2\pi}f(\widehat{\Omega}\cdot n_0)\right]\\ &= \widehat{q}(\vec{r},E)\left[\frac{1}{c}\frac{1}{2\pi}q(\widehat{\Omega}\cdot\widehat{d})\frac{1}{2\pi}f(\widehat{\Omega}\cdot n_0)\right]. \quad (84a)\end{aligned}$$

The constant c is given by

$$c=\int\frac{1}{2\pi}q(\widehat{\Omega}\cdot\widehat{d})\frac{1}{2\pi}f(\widehat{\Omega}\cdot n_0)d\widehat{\Omega}\,. \quad (84b)$$

The birth weights are also a function of direction, where

$$\begin{aligned}w_0(\vec{r},E,\widehat{\Omega}) &= \frac{q(\vec{r},E,\widehat{\Omega})}{\widehat{q}(\vec{r},E,\widehat{\Omega})}\\ &= \frac{R}{\phi^{+}(\vec{r},E)}\frac{2\pi c}{f(\widehat{\Omega}\cdot n_0)}\,, \quad (84c)\end{aligned}$$

as are the target weights

$$\begin{aligned}\overline{w}(\vec{r},E,\widehat{\Omega}) &= \frac{R}{\phi^{\dagger}(\vec{r},E)}\frac{2\pi c}{f(\widehat{\Omega}\cdot n_0)}\\ &= \overline{w}(\vec{r},E)\frac{2\pi c}{f(\widehat{\Omega}\cdot n)}\,. \quad (84d)\end{aligned}$$

Details about how Eqs. (84) were practically implemented are detailed in Ref. 55. The motivated reader may explore this reference for details on the calculation of λ, $\overline{\mu}$, $\left\|J^{\dagger}(\vec{r},E)\right\|$, and $f(\widehat{\Omega}\cdot\widehat{n}_0)$.

VI.A.2.b. Simple Angular CADIS Results

To test these two modifications of CADIS, Peplow et al.[55] ran a number of test problems and compared them against standard implementations of CADIS and analog Monte Carlo runs. For a spherical boat test problem, simple angular CADIS without directional biasing improved the FOM by a factor of 2 to 3. Note that because the source is monodirectional, directional source biasing was not compared. Simple angular CADIS with and without directional source biasing improved the FOM for active interrogation sample problems and for simple duct streaming problems. The methods did not improve the FOMs for sample problems using a neutron porosity tool or a gamma-ray litho-density tool.

The range in performance for angle-dependent problems was explained by Peplow et al.[55] as a failure of the angular flux approximation to capture the true distribution of the angular flux. Because simple angular CADIS uses the same approximation in calculating the angular flux [Eq. (80)] as AVATAR, it is limited in the types of anisotropy that it can capture. As a result, the biasing parameters for a problem are unlikely to adequately reflect the flux distribution in problems where the flux is not captured effectively by the P_1 expansion.

Peplow et al.[55] also noted that because the weight window is dependent on space, energy, and angle, the source birth weights matched the weight window target values only at a specific point in the weight window region. If the weight window covered a substantial region of phase-space, this could result in particle birth weights that do not adequately correspond to the importance of the region into which they are born, resulting in increased run time and a more computationally intensive calculation.

VI.A.3. CADIS-Ω *and FW-CADIS-*Ω

Munk developed an extension of CADIS and FW-CADIS using adjusted scalar fluxes to generate the source biasing and weight window parameters by CADIS and FW-CADIS (Ref. 56). Unlike simple angular CADIS, this method uses the full angular flux solutions. In this case, it uses the adjoint and forward angular fluxes to generate a forward-weighted adjoint scalar flux, as shown in Eq. (85):

$$\phi^{\dagger}_{\Omega}(\vec{r},E)=\frac{\int_{\Omega}\psi^{\dagger}(\vec{r},E,\widehat{\Omega})\psi(\vec{r},E,\widehat{\Omega})d\widehat{\Omega}}{\int_{\Omega}\psi(\vec{r},E,\widehat{\Omega})d\widehat{\Omega}}\,. \quad (85)$$

Then $\phi^{\dagger}_{\Omega}$ is used in place of $\phi^{\dagger}$ in both CADIS and FW-CADIS.

The intention of using a forward-weighted adjoint in CADIS and FW-CADIS is to weight the scalar fluxes—and by extension the source biasing and

weight window values—in regions where the flux is highly anisotropic. In regions where the forward or adjoint fluxes are isotropic, Eq. (85) will result in $\phi^{\dagger}_{\Omega} \approx \phi^{\dagger}$. Only in regions of high anisotropy will the adjusted adjoint flux differ from standard CADIS. Further, because these methods use a scalar flux of the same form as $\phi^{\dagger}$, it could be used in the same manner as $\phi^{\dagger}$ in CADIS and FW-CADIS.

Munk showed that the adjusted formulation of CADIS using the Ω fluxes is given by Eqs. (86). The biased source distribution used by CADIS-Ω is formulated just as it is in CADIS, except the adjusted adjoint fluxes are used:

$$\widehat{q}_{\Omega} = \frac{\phi^{\dagger}_{\Omega}(\vec{r},E)q(\vec{r},E)}{\int\int \phi^{\dagger}_{\Omega}(\vec{r},E)q(\vec{r},E)dEd\vec{r}} = \frac{\phi^{\dagger}_{\Omega}(\vec{r},E)q(\vec{r},E)}{R_{\Omega}} \ . \tag{86a}$$

The starting weights of the particles sampled from the biased source distribution $\widehat{q}$ are given by

$$w_{0,\,\Omega} = \frac{q}{\widehat{q}_{\Omega}} = \frac{R_{\Omega}}{\phi^{\dagger}_{\Omega}(\vec{r},E)} \ , \tag{86b}$$

and the new target weights for the particle are

$$\widehat{w}_{\Omega} = \frac{R_{\Omega}}{\phi^{\dagger}_{\Omega}(\vec{r},E)} \ . \tag{86c}$$

The generalized form for the adjoint source definition is given by the fraction of the response in a region of phase-space P over the total response in the problem, or

$$q^{\dagger}_{\Omega}(P) = q^{\dagger}(P) = \frac{\sigma_d(P)}{R} \ . \tag{87a}$$

When applied to the spatially dependent global dose $\int \phi(\vec{r},E)\sigma_d(\vec{r},E)dE$, the adjoint source will be

$$q^{\dagger}_{\Omega}(\vec{r},E) = q^{\dagger}(\vec{r},E) = \frac{\sigma_d(\vec{r},E)}{\int \sigma_d(\vec{r},E)\psi(\vec{r},E,)dE} \ . \tag{87b}$$

The adjoint source for the spatially dependent total flux $\int \phi(\vec{r},E)dE$ is

$$q^{\dagger}_{\Omega}(\vec{r}) = q^{\dagger}(\vec{r}) = \frac{1}{\int \phi(\vec{r},E)dE} \ . \tag{87c}$$

The adjoint source for the energy-dependent and spatially dependent flux $\phi(\vec{r},E)$ is

$$q^{\dagger}_{\Omega}(\vec{r},E) = q^{\dagger}(\vec{r},E) = \frac{1}{\phi(\vec{r},E)} \ . \tag{87d}$$

Munk implemented both CADIS-Ω and FW-CADIS-Ω in ADVANTG and evaluated the performance of the CADIS-Ω methods on several test problems with varying levels of anisotropy in the neutron flux. Munk designed the problems such that the anisotropy resulted from either interactions with the problem material (e.g., streaming paths) or from a directional source.

When comparing CADIS-Ω to standard CADIS, Munk investigated the impact of the adjusted adjoint flux ϕ_{Ω} on both the deterministic and Monte Carlo calculations. The Ω methods, as implemented in ADVANTG and Denovo, could be quite slow to calculate ϕ_{Ω}. This was due to the large memory requirements for the full angular flux solution for both the forward and the adjoint used to calculate the Ω flux. The method implemented by Munk was neither optimized nor parallelized and was a high cost in the ADVANTG calculation as compared to traditional CADIS and FW-CADIS. In the biased Monte Carlo test problems, the Ω methods yielded varying results. In voids, CADIS and CADIS-Ω performed equivalently well. In some problems CADIS-Ω achieved a FOM an order of magnitude larger than standard CADIS. In others, CADIS-Ω performed poorly. In almost all cases CADIS-Ω achieved lower relative errors than standard CADIS. Conversely, the Monte Carlo runs biased by CADIS-Ω took longer to run than standard CADIS. The combination of longer run times but lower relative errors resulted in varying performance of CADIS-Ω. Munk observed no trend with anisotropy and the success of the method.

VI.A.4. Cooper's Weight Windows

Cooper and Larsen, in addition to generating global isotropic weight windows from a deterministic forward solution (as described in Sec. V.A), also developed angle-dependent weight windows.[36] Here, the forward angular

flux is calculated in a similar manner as the AVATAR method, where the angular flux is a product of the scalar flux and an angle-dependent function. In this case, the adjustment factor also includes a factor of 4π:

$$\psi(\vec{r},\widehat{\Omega}) \approx A(\vec{r})e^{\vec{B}(\vec{r})\cdot\widehat{\Omega}} , \tag{88a}$$

where $A(\vec{r})$ and $\vec{B}(\vec{r})$ are given by

$$A(\vec{r}) = \frac{\phi(\vec{r})}{4\pi}\frac{B(\vec{r})}{\sinh B(\vec{r})} , \tag{88b}$$

$$\vec{B}(\vec{r}) = B(\vec{r})\frac{\vec{\lambda}(\vec{r})}{\left|\vec{\lambda}(\vec{r})\right|} , \tag{88c}$$

and

$$\lambda(\vec{r}) = \coth B(\vec{r}) - \frac{1}{B(\vec{r})} . \tag{88d}$$

If both $A(\vec{r})$ and $\vec{B}(\vec{r})$ are inserted into Eq. (88a), the formulation will be very similar to AVATAR's reconstruction of the angular flux. However, Cooper's method differs from AVATAR in the calculation of $\lambda(\vec{r})$. Cooper noted that $\lambda(\vec{r})$ could be estimated either with the scalar fluxes and currents from a fairly low-cost quasi-diffusion calculation,

$$\begin{aligned}\lambda_i(\vec{r}) &= \frac{J_i(\vec{r})}{\phi(\vec{r})}, \quad 1 \le i \le 3 \\ &= \frac{1}{\Sigma_{tr}(\vec{r})\phi(\vec{r})}\frac{\partial}{\partial r_j}E_{ij}(\vec{r})\phi(\vec{r}) ,\end{aligned} \tag{88e}$$

or with the scalar fluxes and currents directly from the Monte Carlo solution [$E_{ij}(\vec{r})$ is the Eddington factor described in Sec. V.A]. Cooper noted that because Monte Carlo robustly calculates the Eddington factor, the current, and the scalar flux, it is the more optimal choice, though it is more computationally expensive than the quasi-diffusion calculation. After obtaining the current and scalar flux values (with which to calculate λ_i) from the chosen method, Cooper's angle-dependent weight window could be calculated for each cell i,j with

$$ww_{i,j}(\widehat{\Omega}) = \frac{\psi_{i,j}(\vec{r},\widehat{\Omega})}{\max\phi_{i',j'}/4\pi} , \tag{88f}$$

where $\max\phi_{i',j'}$ is the maximum scalar flux in the system.

As mentioned in Sec. V.A, Cooper's method was limited in that it used an iterative quasi-diffusion/Monte Carlo solution to generate the biasing parameters for the problem. This method was not automated, and the ideal frequency between iterations was never explored. However, Cooper showed in two-dimensional (2-D) example problems that the angularly dependent weight windows significantly improved the FOM as compared to analog Monte Carlo. The distributions of the FOM and the resulting tally were also much smoother with the approach described in their work. Further, the angular weight windows performed slightly better than the isotropic weight windows in evenly distributing the particles, even in problems where the anisotropy was not significant. However, like AVATAR, this method is limited in the types of anisotropy it can quantify as a result of the approximations it uses to reconstruct the angular flux. In generating the estimates for $\vec{\lambda}$, Cooper found that using a quasi-diffusion estimate was more efficient than using Monte Carlo estimates, likely because the estimates of the factors could be periodically updated as the solution iteratively converged.

VI.A.5. Lagrange Discrete Ordinates with CADIS and FW-CADIS

Many of the angle-informed hybrid methods described in Sec. VI have used approximations of the angular flux to construct angle-informed VR parameters. The methods are limited by the quality of the solution used to generate such parameters. The resolutions of space, energy, and angle all play a role in the quality of the solution, and in turn, each affects the time to converge on an acceptable solution. When ray effects are present in the deterministic solution, for example, they will be propagated into the biasing parameters of the Monte Carlo simulation. Rowland et al. studied the use of an alternative formulation of the transport equation, the Lagrange Discrete Ordinates[57] (LDO) equations, for use in CADIS and FW-CADIS. The LDO formulation has a number of favorable features that make it a potentially attractive method with which to generate the adjoint fluxes in problems with strong angular anisotropy. The quadrature set can be rotated arbitrarily, so a problem with poor performance due to a particular quadrature interface can be remedied with a rotation in the quadrature set. Further, solutions obtained by solving the LDO equations allow for interpolation between the quadrature

points, so a user could get the flux for any arbitrary point in the unit sphere described by the quadrature set. While the LDO formulation has a number of attractive features, Rowland et al. did not deeply investigate the effect of either of these features on the performance of CADIS or FW-CADIS using a deterministic solution with an LDO quadrature set.

Rowland implemented the LDO equations in Denovo and performed a study to see if it produced favorable results in problems with strong angular anisotropy.[58] Rowland used the CADIS and FW-CADIS methods implemented in ADVANTG to bias Monte Carlo simulations with MCNP. In this study it was found that the LDO equations performed well in problems with photons, likely due to the number of scattering coefficients available, which allowed for a favorable representation of the physics with a low-order quadrature set. The LDO construction did not appear to have consistently superior performance to other quadrature sets in S_N for neutron transport. Rowland's work, however, offers a number of interesting possibilities for future work in angular-informed hybrid methods. For example, solutions of the LDO equation solutions could be used to construct VR parameters with methods using the exponential transform (Sec. VI.B). The LDO equations were not tested using angular weight windows, which classically have a high computational cost and unnecessary burden for VR. However, the nature of the LDO quadrature sets may allow for explicit angle-dependent weight windows to be constructed from its solution.

VI.B. Angular Biasing Using the Exponential Transform

VI.B.1. Early Work

As discussed in Sec. II.B, the exponential transform is a modified sampling method that adjusts the distance to collision in Monte Carlo transport to encourage particle transport in preferential regions. This is done by modifying the sampled cross section. Recall from Eq. (25) that the exponential transform is dependent on a transform parameter p and the cosine angle μ such that $\Sigma_t^* = \Sigma_t(1 - p\mu)$. When used without angle biasing,

$$\psi_g^\dagger(r, \Omega) \approx e^{\Sigma_t \lambda \cdot r} , \tag{89}$$

the exponential transform can have undesirable weight fluctuations,[33] especially as the number of collisions to reach a tally increases.[59] Equation (89) shows that the importance function (the adjoint flux) can be approximated as an exponential function varying in space, dependent on the total cross section Σ_t, distance traveled r, and a parameter defining the amount and direction of biasing λ.

Dwivedi[60] showed that by adding an angle-dependent collision biasing scheme in addition to the exponential transform, the problematic weight fluctuations could be mitigated. The collision biasing scheme introduced with the exponential transform takes the form

$$\psi_g^\dagger(r, \Omega) \approx \frac{\sigma_{s,0} e^{\Sigma_t \lambda \cdot r}}{4\pi\sigma_t(1 - \lambda \cdot \Omega)} . \tag{90}$$

Note that the ratio of cross sections outside of the exponential function $\sigma_{s,0}/\sigma_t$, where $\sigma_{s,0}$ is the zeroth moment of the scattering cross section, is the survival probability in an interaction event, and the $(1 - \lambda \cdot \Omega)$ term is consistent with the weight adjustment required for the exponential transform [Eq. (26)]. This was applied to a monoenergetic problem with slab geometry and isotropic scattering, and the variance was reduced by a factor of more than 100 when compared with other exponential transform methods.

Gupta and Dwivedi's subsequent work[59] adjusted the factor described in the preceding paragraph by applying the exponential transform with angle biasing to deep-penetration problems with anisotropic scattering. Gupta and Dwivedi did not explicitly use the true distribution for anisotropic scattering but rather chose to approximate the biased kernel to be a function of the isotropic angular distribution. They observed a reduction in the variance by a factor of 10, but they acknowledged that while the combination of the biased kernel and exponential biasing reduced weight fluctuations, it also had the potential to introduce other weight fluctuations due to anisotropies in the flux.

Ueki and Larsen[61] generalized Dwivedi's importance transform and applied it to isotropic, linearly anisotropic, and quadratically anisotropic scattering. They observed that Dwivedi's method and the generalized Dwivedi method outperformed non-angle-dependent exponential biasing for all types of scattering and that Ueki and Larsen's generalized method outperformed Dwivedi's original method in higher-order scattering. The works of Dwivedi, Gupta and Dwivedi, and Ueki and Larsen were applied and each compared with 1-D sample problems. Ueki and Larsen pointed out that their method could be extended to three-dimensional problems using Turner and Larsen's methodology (described in Sec. VI.B.2, Ref. 61).

In 1985, Hendricks and Carter[62] described a method by which photon transport could be biased in angle with an exponential transform adjustment factor. They performed studies on three test problems with the exponential transform adjustment factor and with a synergistic angular bias and exponential transform adjustment. In all studies, the synergistic biasing outperformed the exponential transform adjustment alone. However, their method performed best in highly absorbing media. They noted that this performance was because the biasing could be strong without undersampling scattering in the problem. They also pointed out that while the weight window method was comparable in efficiency to the method described, their method avoided choosing importances and weight window values for biasing. Their method was limited to exclusively photon transport biasing and not neutron transport. However, Hendricks and Carter were optimistic that the method could be extended to neutron transport with relative ease. Both et al.[63] also derived VR parameters for the exponential transform and for collision biasing based on the adjoint solution as a measure of importance.

VI.B.2. Local Importance Function Transform

The Local Importance Function Transform[64,65] (LIFT) method developed by Turner and Larsen, like Dwivedi's exponential transform, is a modification of the zero variance solution (see Sec. III.C). Consequently, the LIFT method uses a calculation of the adjoint flux as a measure for importance in the problem to distribute particles according to the contributon density in the problem. LIFT uses a deterministic calculation to generate biasing parameters for the exponential transform and weight window VR techniques.

As with the form of the importance function derived by Dwivedi [Eq. (90)], the LIFT method generates an angle-dependent importance function by taking the product of a space-based exponential function and an angle-informed collision estimator. Additionally, LIFT uses a deterministic calculation of the adjoint scalar flux to inform the angular flux reconstruction. The adjoint angular flux is approximated as piecewise continuous in space and angle with Eqs. (91a) through (91d):

$$\psi^{\dagger}_{g,n}(r,\Omega) \approx \phi^{\dagger}_{g,n} V_n \left[\beta_{g,n} \frac{\sigma_{s_0,g\to g,n} b_{g,n}(\Omega)}{\sigma_{t,g,n} - \rho_{g,n}\cdot\Omega} e^{\rho_{g,n}\cdot(r-r_n)} \right] , \tag{91a}$$

where the physical system comprises N regions of volume V_n and $\psi^{\dagger}_{g,n}$ is the approximation of the adjoint angular flux for group g and region n. Further, β, the normalization factor, is given by

$$\beta_{g,n} = \frac{1}{\int_{V_n} e^{\rho_{g,n}\cdot(r-r_n)} dr \int_{4\pi} \frac{\sigma_{s_0,g\to g,n} b_{g,n}(\Omega)}{\sigma_{t,g,n} - \rho_{g,n}\cdot\Omega} d\Omega} , \tag{91b}$$

where $b_{g,n}$, the linearly anisotropic factor, is

$$b_{g,n}(\Omega) = 1 + 3\mu_{g\to g,n} \frac{\sigma_{t,g,n} - \sigma_{s_0,g\to g,n}}{\left|\rho_{g,n}\right|^2} \rho_{g,n}\cdot\Omega, \tag{91c}$$

and the biasing parameter $\rho_{g,n}$ is given by the product of the cross section and the biasing parameter λ seen previously in Eqs. (89) and (90):

$$\rho_{g,n} = \sigma_{t,g,n}\lambda_{g,n} . \tag{91d}$$

Turner and Larsen showed that $\rho_{g,n}$ can be obtained from the deterministic solution to the adjoint equation rather than from the cross section and λ, which requires some assumptions on the distribution of particles. Turner and Larsen's corresponding solutions for ρ in terms of the deterministic scalar fluxes are

$$\rho_{i,g,n} = \frac{1}{\Delta x_n} \ln\left(\frac{\phi^{\dagger}_{g,i+1/2}}{\phi^{\dagger}_{g,i-1/2}} \right) , \tag{92a}$$

$$\rho_{j,g,n} = \frac{1}{\Delta y_n} \ln\left(\frac{\phi^{\dagger}_{g,j+1/2}}{\phi^{\dagger}_{g,j-1/2}} \right) , \tag{92b}$$

and

$$\rho_{k,g,n} = \frac{1}{\Delta z_n} \ln\left(\frac{\phi^{\dagger}_{g,k+1/2}}{\phi^{\dagger}_{g,k-1/2}} \right) . \tag{92c}$$

Each value of ρ is defined using cell-edge flux values in Cartesian coordinates.

Equation (91a) is an adjustment of the exponential transform described by Dwivedi.[60] However, rather than relying upon an isotropic scattering law, like earlier implementations of the exponential transform, the LIFT

method adjusts the transform to instead be linearly anisotropic in angle. The derivation of this equation for both linearly anisotropic scattering and isotropic scattering is available in Ref. 64. To summarize, the parameters $\beta_{g,n}$, $b_{g,n}$, and $\rho_{g,n}$ are calculated from values obtained from the deterministic calculation and are used to calculate $\psi^{\dagger}_{g,n}$.

In addition to using the exponential transform to bias the particles in angle, the LIFT method also uses weight windows for particle weight adjustment. However, the computational cost of generating angle-dependent weight windows from the previous equations led Turner and Larsen to choose space-energy exclusive weight windows. The weight window target values were calculated to be inversely proportional to the adjoint solution, as with other methods:

$$ww_{center,g,n} = \frac{\phi^{\dagger}_{g,src}}{\phi^{\dagger}_{g,n}} \ . \tag{93}$$

The LIFT method,[64,65] like AVATAR, calculated the angular flux for a region by assuming the angular flux was a product of the scalar flux and an exponential function. The angular flux values were then used to generate values for the exponential transform VR technique to bias the particles in space, energy, and angle. Like AVATAR, LIFT also generated weight window parameters. However, generating a full angle-dependent weight window map and running Monte Carlo transport with those weight windows was computationally limiting, and Turner and Larsen chose to generate only space- and energy-dependent weight windows. They showed that LIFT outperformed AVATAR for several example problems, but both methods performed poorly in voids and low-density regions.

Turner and Larsen compared a number of variants of LIFT (Ref. 65) against AVATAR to determine the efficiency of LIFT. In their investigation, Turner and Larsen compared LIFT and AVATAR using approximations for the adjoint solution with diffusion and S_N transport calculations, and with various methods to calculate weight window parameters, including using LIFT combined with AVATAR's weight window parameters. In most cases, LIFT outperformed AVATAR. In problems with voids and low-density regions, the efficiency of the LIFT method decreased, but so did AVATAR. This independently confirmed the findings of the previous study. However, an important note that Turner and Larsen mentioned was that while increasing the accuracy of the deterministic solution may decrease the variance, it is not necessarily the best for the FOM. This is a valuable lesson for all automated VR methods: An overly accurate solution for the adjoint problem may reduce the variance but may come at such a high computational cost that it decreases the FOM.

More recently, Keady and Larsen showed that LIFT could be improved upon further by using cell-averaged currents and fluxes rather than cell-edge values for angular biasing.[66] By using this modified variation of LIFT, material interfaces do not create strong flux discontinuities on cell edges, resulting in a solution that is both smoother and more realistic. Results were presented for a 1-D monoenergetic slab problem with material interfaces. The modified version of LIFT outperformed both the original LIFT method and Monte Carlo weight windows generated with forward deterministic weight windows.

VII. OTHER VR METHODS

Sections IV, V, and VI describe a number of efforts to reduce the variance in Monte Carlo problems according to different problem constraints: localized detectors, global tallies, or problems requiring additional angular information. However, there exist a few methods that are not well described using the previous classifiers.

Becker and Larsen[67] developed a general transform for VR. Their general transform is applicable to many different types of VR methods, including source biasing, weight windows, the exponential transform, or collision biasing. It is also valid in space, energy, and angle, thus applying to any of the aforementioned sections of this paper. This general transform allows for VR parameters to be determined for any Monte Carlo particle distribution, which allows the user flexibility in choosing a distribution (and VR parameters) that is problem dependent.

Becker and Larsen's general transform defines the angular flux in terms of a transform function T, the weight window centers w, and the Monte Carlo particle flux m:

$$\psi(x,\Omega,E) = T(x,\Omega,E)w(x,\Omega,E)m(x,\Omega,E) \ . \tag{94}$$

The full derivation of Eq. (94) can be found in Ref. 67.

By combining a transform function and a weight window, a user can use any combination of VR methods to distribute particles throughout the problem given a particular particle distribution. The user may choose

to use only the transform function, only weight windows, or some combination of both to achieve the desired particle distribution in the problem. For example, should the user choose to use exclusively weight windows, the transform function T can be set to 1, and Eq. (94) reduces to

$$\psi(x,\Omega,E) = w(x,\Omega,E)m(x,\Omega,E) \ . \tag{95}$$

If the weight window center is chosen such that $w(x,\Omega,E) = 1/\psi^{\dagger}(x,\Omega,E)$, as is common in many of the previously mentioned VR methods, the Monte Carlo particle distribution in the problem becomes

$$m(x,\Omega,E) = \psi(x,\Omega,E)\psi^{\dagger}(x,\Omega,E) \ . \tag{96}$$

This resultant particle distribution, the contributon flux, is observed in methods using the adjoint flux in the weight window values.

Conversely, if a user chooses to bias with no weight windows and a transform function alone, w may be set to 1, and Eq. (94) reduces to

$$\psi(x,\Omega,E) = T(x,\Omega,E)m(x,\Omega,E) \ . \tag{97}$$

One may note that this derivation of the general transform also allows one to determine what the particle distribution in the problem will be, given a set of weight windows. This method allows for any particle distribution to be chosen by the user, and then any combination of the transform function and weight window values can be combined to achieve that distribution.

Becker and Larsen applied the general transform to two demonstration problems representative of those commonly encountered in hybrid methods: a global flux problem and a source-detector problem. The general transform was applied to these problems at both extremes, using either the complete transform function or the weight window. Both variations of the general transform function yielded comparable results.

All of the methods presented in Secs. III though VI moved particles in the system according to some choice, whether that be the adjoint flux, the contributon flux, or something else. Our choice of particle distribution has classically been with the intent of reducing the FOM by increasing the particle population in tally regions. However, Becker and Larsen showed that there is no rigorous mathematical link between the FOM and the Monte Carlo particle distribution, though the improvement in the FOM from a higher particle population is observable.

Solomon et al.[68] proposed a method to optimize the FOM by calculating the tally variance and the average computational time per history, thereby directly optimizing the FOM. This method is called the Cost Optimized Variance Reduction Technique (COVRT). Solomon et al. showed that the history-score moment equations describe the moments of a Monte Carlo tally score distribution. The first two moments of the history-score moment equations can be used to calculate the tally variance. Additionally, the future time equation can be solved to determine the average computational time per history. Together, these can be combined for a deterministic estimate of the Monte Carlo FOM.

Solomon et al. deterministically obtained solutions for the history-score moment equations and the future time equations using a discrete ordinates method. The solutions were then used to calculate the cost to achieve a desired solution. Weight window bounds were chosen such that the cost function was minimized, that is, that the trade-off between the tally variance and the average particle time in the solution was optimized. Solomon et al. applied this methodology to 1-D and 2-D problems and observed improvements in the FOM by up to a factor of 2 as compared to standard adjoint-based VR. Solomon et al. also compared the weight window maps generated by standard adjoint-based methods to the COVRT method and found that COVRT generated weight window values that differed by up to a factor of 2.

Kulesza et al.[69] performed an assessment of the COVRT method on several 1-D and 2-D test problems with weight-dependent and weight-independent parameters. One may recall from Sec. II.B that some VR methods are dependent on particle weight (weight windows) and others are not (splitting and rouletting). Solomon et al.'s initial work generated weight-dependent VR parameters, but the methodology is also valid for generating weight-independent parameters. Kulesza compared weight-dependent and weight-independent COVRT-biased Monte Carlo with unbiased Monte Carlo. Kulesza's initial work found that COVRT improved the FOM as compared to unbiased Monte Carlo and also had a higher FOM than ADVANTG for a single test problem. However, when comparing COVRT and ADVANTG, the deterministic solution took orders of magnitude longer with COVRT than ADVANTG. This was attributed to the production-level algorithmic implementation of the deterministic solver used by ADVANTG as compared to the research code used by COVRT. Kulesza then extended the COVRT method to be usable with DXTRAN (Ref. 70) in one and two dimensions. COVRT was found to generate good parameters in this case.

VIII. VARIANCE REDUCTION IN LARGE APPLICATION PROBLEMS

Variance reduction methods exist for Monte Carlo methods to achieve a more accurate answer in a shorter amount of time. Automated VR methods have been designed to aid users in generating VR parameters where it might not be intuitive or obvious what VR parameters are best for a problem. The most successful VR methods construct or estimate an importance function for the desired response from a preliminary calculation. This importance function may be derived from the adjoint solution to the transport equation, or it may be derived from contributon theory.

The methods described in Secs. IV, V, and VI have been implemented and tested in a number of software packages. The problem spaces over which they have been applied are extensive and show that a large subset of application problems can be successfully simulated with the assistance of existing VR techniques. Local VR methods can be used to reduce the variance in source-detector problems where the detector constitutes a small subset of the problem phase-space. Global VR methods can be used to distribute response sampling equally throughout several tallies or a problem-wide tally. Angle-based VR methods are used in problems where space and energy VR methods alone are not sufficient. For large and complex problems, automated versions of each of these methods are required as the user expertise to obtain even remotely adequate parameters is significant. Here, the existing state of automated VR methods and the applications on which they have been tested will be summarized.

At present, numerous hybrid method packages that use the methods described in Secs. IV, V, and VI are available. These packages are targeted toward deep-penetration radiation transport and shielding applications. The CADIS and FW-CADIS methods are distributed with MAVRIC (Refs. 23 and 40) and ADVANTG (Ref. 71) from Oak Ridge National Laboratory (ORNL), which use the Denovo discrete ordinates code[72] to make VR parameters for the Monte Carlo codes Monaco (Ref. 23) and MCNP (Ref. 2), respectively. CADIS and FW-CADIS are also available in the Tortilla code,[73] which uses the hybrid method software using the Attilla deterministic code.[74] Tortilla also includes a version of LIFT and LIFT-based weight windows. The Deterministic Adjoint Weight Window Generator (DAWWG) from Los Alamos National Laboratory[75] uses the adjoint solution from a deterministic solve in PARTISN (Ref. 76) to generate biasing parameters for MCNP and also includes AVATAR functionality. MCNP (Ref. 2) is distributed with a WWG that uses a preliminary Monte Carlo solution to estimate an importance function for the problem. Though this list is not exhaustive, it illustrates the present ubiquity and need for hybrid methods to analyze realistic problems. In the analysis of realistic problems, ensuring that a "good" answer is achieved is necessary for safety and security. In the next few paragraphs, how and how effectively each of these methods have been applied to application problems is summarized. The degree to which each is successful is also discussed.

CADIS and FW-CADIS have been used for a number of studies of spent fuel storage facilities. Radulescu et al. used FW-CADIS in MAVRIC to calculate spent fuel dose rates of a single dry cask with finely detailed geometry and spent fuel isotopic compositions.[77] Chen et al. used MAVRIC (Ref. 23) to analyze dose rates on spent fuel storage containers.[78] The fueled region of the storage container was homogenized into an effective fuel region. They found that in a coarse energy group calculation, MAVRIC underestimated neutron dose rates at high energies. However, MAVRIC's ability to generate importances in three dimensions allowed it to have better problem-wide results, while other methods (SAS4) struggled to generate satisfactory results in the axial direction. This was demonstrated to a greater extent in an analysis of an independent spent nuclear fuel storage installation[79] (ISFSI) by Sheu et al. The FOM achieved by MAVRIC appeared inferior to that obtained with SAS4 or TORT/MCNP in a single cask. However, when applied to a storage bed of 30 casks, MAVRIC was able to generate VR parameters, which were unfeasible for the other two methods. These studies demonstrated that CADIS and FW-CADIS are desirable methods for which to obtain global and three-dimensional VR parameters for realistic problems.

ADVANTG (Ref. 71), developed at ORNL (Refs. 34, 80, and 81), is a hybrid method package for automated VR of the Monte Carlo transport package MCNP (Ref. 4). ADVANTG uses the Denovo deterministic transport code[72] to perform the forward and adjoint calculations for CADIS and FW-CADIS. At its inception, ADVANTG was used to analyze various threat detection nonproliferation problems.[71] FOM improvements on the order of 10^2 to 10^4 when compared with analog Monte Carlo have been observed. However, Mosher et al. noted that the methods struggled with problems exhibiting strongly anisotropic behavior. In particular, they noted that low-density materials and strongly directional sources

posed issues. This indicated that while CADIS and FW-CADIS are very useful methods, they have limitations in highly angle-dependent applications.

DAWWG utilizes the PARTISN discrete ordinates code[75] to generate space- energy-, and angle-dependent weight windows. It is an internal feature of MCNP. The angle-dependent weight windows are calculated with the same methodology as AVATAR (Refs. 12 and 75). Sweezy et al. compared DAWWG to the standard MCNP WWG on an oil well logging problem, a shielding problem, and a dogleg neutron void problem. DAWWG obtained similar relative errors as the standard WWG for the first two problems but in a fraction of the time. However, for the dogleg void problem, which exhibited strong angular dependence in the neutron flux, Sweezy et al. noted that DAWWG was not as effective as the standard MCNP WWG. This was attributed to ray effects from the S_N transport influencing the weight windows obtained by DAWWG, which is not an issue for the standard WWG.

A variety of automated VR methods, including CADIS and LIFT, have been implemented into the Attila/Tortilla deterministic and hybrid transport code packages.[73] These methods were used on several nonproliferation test problems. For the most part, LIFT and LIFT combined with weight windows outperformed CADIS's weight windows and source biasing, indicating that the addition of angular information was of benefit for these more realistic nonproliferation application problems.

Peplow et al. formulated an adjustment to CADIS in the ORNL code suite[55] to incorporate angular information into the VR parameters (see Sec. VI.A.2). Two different methods to generate weight windows and source biasing parameters were investigated: CADIS with directional source biasing and CADIS without directional source biasing. For the method without directional source biasing, the biased source distribution matched that of the original CADIS, but the weight window values were directionally dependent. The method with directional source biasing used the transform function to obtain directionally dependent weight windows and directional source biasing. Peplow et al. found that these methods generally increased the FOM by up to a factor of 5 as compared to traditional CADIS but in some cases decreased the FOM. This was attributed to the P_1 approximation used to calculate the angular flux, which limited the physical applicability of the method, just as with AVATAR.

CADIS and FW-CADIS have become the existing gold standard of local and global VR methods for large application problems, a selection of which are described in the preceding paragraphs. These problems include active interrogation of cargo containers,[71] spent fuel storage casks[77,78] and storage facilities (ISFSI) (Ref. 79), and other nonproliferation and shielding applications.[73] For additional applications, one may refer to Ref. 34. In some of these application problems, the parameters generated by CADIS or FW-CADIS were sufficient for the problem application. However, for other problems that had strong angular dependence or geometric complexity, the parameters were insufficient.[55,73,78] This can be remedied with additional angular information in the VR parameters, such as LIFT (Ref. 73), but the benefits of consistent source biasing are lost in this case. Alternatively, the angular flux can be reconstructed in a manner similar to AVATAR (Refs. 55 and 75) to generate angle-dependent weight windows, but this approximates the angular flux to be linearly anisotropic in angle (from the P_1 reconstruction) and is also dependent on the deterministic flux not having ray effects.[75]

Although numerous methods have been proposed and implemented to obtain adequate angle-informed VR parameters for application problems, they have limited applicability, and determining in which problems they will be useful is not always straightforward. No single method has been successful for problems with all types of anisotropy, and no existing angle-informed method captures the anisotropy in the flux without significant approximation. For large-scale, highly anisotropic, deep-penetration radiation transport problems, there exists a need for improvements in hybrid methods.

IX. CONCLUSIONS

Hybrid methods are and will be a realm of continued importance in radiation transport method development. The application space and demand for hybrid methods continues to grow. With this growth, accurately and efficiently modeling the physics of increasingly complex problems is paramount for safety and security.

Acknowledgments

We are grateful for the strong field of method development and method developers that necessitated this review. In particular, Tara Pandya, Seth Johnson, Steven Hamilton, and Tom Evans at ORNL have been instrumental for us. We would also like to thank Ed Larsen for graciously providing his personal notes on contributon theory to supplement our understanding of the material. Last, Kathryn Huff was indispensable in preparing this manuscript from its original form as a dissertation chapter. We are grateful for her contribution to this work and her help in getting this manuscript in its

current form. Critical review of this review came from Massimiliano Fratoni, Tara Pandya, and John Harte in its early stage. Time to prepare this publication was supported in part by the Gordon and Betty Moore Foundation's Data-Driven Discovery Initiative through grant GBMF4561 to Matthew Turk. This material is based on work supported by the U.S. Department of Energy under award number DE-NE 0008286.

ORCID

Madicken Munk http://orcid.org/0000-0003-0117-5366
Rachel N. Slaybaugh http://orcid.org/0000-0002-6296-6519

References

1. E. E. LEWIS and W. F. MILLER, *Computational Methods of Neutron Transport*, John Wiley and Sons, Inc., New York (1984).
2. X-5 MONTE CARLO TEAM, "MCNP—A General N-Particle Transport Code, Version 5, Volume I: Overview and Theory," LA-UR-03-1987, Los Alamos National Laboratory (2003).
3. F. B. BROWN et al., "MCNP Version 5," *Trans. Am. Nucl. Soc.*, **87**, 273 (2002).
4. X-5 MONTE CARLO TEAM, "MCNP—A General N-Particle Transport Code, Version 5, Volume II: Users Guide," LA-CP-03-0245, Los Alamos National Laboratory (2003).
5. J. S. HENDRICKS and T. E. BOOTH, "MCNP Variance Reduction Overview," *Monte-Carlo Methods and Applications in Neutronics, Photonics and Statistical Physics*, pp. 83–92, Springer; (1985) http://link.springer.com/chapter/10.1007/BFb0049037 (current as of Dec. 7, 2018).
6. T. E. BOOTH, K. C. KELLEY, and S. S. McCREADY, "Monte Carlo Variance Reduction Using Nested Dxtran Spheres," *Nucl. Technol.*, **168**, *3*, 765 (2009); https://doi.org/10.13182/NT09-A9303.
7. T. E. BOOTH, "Automatic Importance Estimation in Forward Monte Carlo Calculations," *Trans. Am. Nucl. Soc.*, **41**, 308 (1982); http://inis.iaea.org/search/search.aspx?orig_q=RN:14757371 (current as of Dec. 7, 2018).
8. J. S. HENDRICKS, "A Code-Generated Monte Carlo Importance Function," *Trans. Am. Nucl. Soc.*, **41**, 307 (1982); http://inis.iaea.org/search/search.aspx?orig_q=RN:14753414 (current as of Dec. 7, 2018).
9. T. E. BOOTH and J. S. HENDRICKS, "Deep Penetration by Monte Carlo," *Trans. Am. Nucl. Soc.*, **43**, 609 (1982); http://www.osti.gov/scitech/biblio/6041526 (current as of Dec. 7, 2018).
10. T. E. BOOTH and J. S. HENDRICKS, "Importance Estimation in Forward Monte Carlo Calculations," *Fusion Sci. Technol.*, **5**, *1*, 90 (1984); http://epubs.ans.org/?a=23082 (current as of Dec. 7, 2018).
11. T. M. EVANS and J. S. HENDRICKS, "An Enhanced Geometry-Independent Mesh Weight Window Generator for MCNP," LA-UR-97-5057, Vol. 1, p. 165, Los Alamos National Laboratory (1998); https://www.osti.gov/scitech/biblio/663177 (current as of Dec. 7, 2018).
12. K. A. VAN RIPER, "Generation of a Monte Carlo Variance Reduction Map from a Deterministic Transport Calculation," LA-UR-95-0747, Los Alamos National Laboratory (1995).
13. T. E. BOOTH, "Common Misconceptions in Monte Carlo Particle Transport," *Appl. Radiat. Isot.*, **70**, *7*, 1042 (2012); https://doi.org/10.1016/j.apradiso.2011.11.037.
14. J. LEWINS, *Importance: The Adjoint Function. The Physical Basis of Variational and Perturbation Theory in Transport and Diffusion Problems*, North-Holland Publishing Company, Amsterdam (1966); http://www.osti.gov/scitech/biblio/4752764 (current as of Dec. 7, 2018).
15. J. LEWINS, "Developments in Perturbation Theory," *Adv. Nucl. Sci. Technol.*, **4**, 309 (1968).
16. E. GREENSPAN, "Developments in Perturbation Theory," *Adv. Nucl. Sci. Technol.*, **9**, 181 (1976).
17. I. LUX and L. KOBLINGER, *Monte Carlo Particle Transport Methods: Neutron and Photon Calculations*, CRC Press, Boca Raton, Florida (1991).
18. G. GOERTZEL and M. H. KALOS, "Monte Carlo Methods in Transport Problems," *Prog. Nucl. Energy*, **2**, 315 (1958).
19. M. H. KALOS, "Importance Sampling in Monte Carlo Shielding Calculations: I. Neutron Penetration Through Thick Hydrogen Slabs," *Nucl. Sci. Eng.*, **16**, *2*, 227 (1963); https://doi.org/10.13182/NSE63-A26504.
20. R. R. COVEYOU, V. R. CAIN, and K. J. YOST, "Adjoint and Importance in Monte Carlo Application," *Nucl. Sci. Eng.*, **27**, *2*, 219 (1967); https://doi.org/10.13182/NSE67-A18262.
21. J. S. TANG and T. J. HOFFMAN, "Monte Carlo Shielding Analyses Using an Automated Biasing Procedure," *Nucl. Sci. Eng.*, **99**, *4*, 329 (1988); https://doi.org/10.13182/NSE88-A23562.
22. N. M. GREENE and L. M. PETRIE, "XSDRNPM-S: A One-Dimensional Discrete-Ordinates Code for Transport Analysis," NUREG/CR–0200-VOL.2, Oak Ridge National Laboratory (1984); http://inis.iaea.org/Search/search.aspx?orig_q=RN:17040287 (current as of Dec. 7, 2018).
23. B. T. REARDEN and M. A. JESSEE, "SCALE Code System," ORNL/TM-2005/39, Version 6.2.1, Oak Ridge

National Laboratory (2016); https://rsicc.ornl.gov/codes/ccc/ccc8/ccc-834.html (current as of Dec. 7, 2018).

24. M. L. WILLIAMS, "Generalized Contributon Response Theory," *Nucl. Sci. Eng.*, **108**, *4*, 355 (1991); https://doi.org/10.13182/NSE90-33.
25. M. L. WILLIAMS and H. MANOHARA, "Contributon Slowing-Down Theory," *Nucl. Sci. Eng.*, **111**, *4*, 345 (1992); http://www.ans.org/pubs/journals/nse/a_15483 (current as of Dec. 7, 2018).
26. M. L. WILLIAMS, "A Fundamental Study of Contributon Transport Theory and Channel Theory Applications," DOE/ER/12899–T1, Louisiana State University (1994).
27. T. L. BECKER, "Hybrid Monte Carlo/Deterministic Methods for Deep-Penetration Problems," PhD Dissertation, University of Michigan (2009).
28. M. L. WILLIAMS and W. W. ENGLE, "The Concept of Spatial Channel Theory Applied to Reactor Shielding Analysis," ORNL/TM-5467, Oak Ridge National Laboratory (1976).
29. M. L. WILLIAMS, "The Relations Between Various Contributon Variables Used in Spatial Channel Theory," *Nucl. Sci. Eng.*, **63**, *2*, 220 (1977); https://doi.org/10.13182/NSE77-A27033.
30. M. SEYDALIEV and D. L. HENDERSON, "Contributon Theory for Shielding Analysis," University of Wisconsin, Fusion Technology Institute (2008); http://icf4.neep.wisc.edu/pdf/fdm1338.pdf (current as of Dec. 7, 2018).
31. J. C. WAGNER and A. HAGHIGHAT, "Automatic Variance Reduction for Monte Carlo Shielding Calculations with the Discrete Ordinates Adjoint Function," *Proc. Joint Int. Conf. Mathematical Methods and Supercomputing for Nuclear Applications*, Saratoga Springs, New York, October 5–9, 1997, Vol. 1, p. 67, American Nuclear Society (1997).
32. J. C. WAGNER and A. HAGHIGHAT, "Automated Variance Reduction of Monte Carlo Shielding Calculations Using the Discrete Ordinates Adjoint Function," *Nucl. Sci. Eng.*, **128**, *2*, 186 (1998); https://doi.org/10.13182/NSE98-2.
33. A. HAGHIGHAT and J. C. WAGNER, "Monte Carlo Variance Reduction with Deterministic Importance Functions," *Prog. Nucl. Energy*, **42**, *1*, 25 (2003); http://www.sciencedirect.com/science/article/pii/S0149197002000021 (current as of Dec. 7, 2018).
34. J. C. WAGNER et al., "Review of Hybrid (Deterministic/Monte Carlo) Radiation Transport Methods, Codes, and Applications at Oak Ridge National Laboratory," *Prog. Nucl. Sci. Technol.*, **2**, 808 (2011); https://doi.org/10.15669/pnst.2.808.
35. J. C. WAGNER, "An Automated Deterministic Variance Reduction Generator for Monte Carlo Shielding Applications," *Proc. 12th Biennial Topl. Mtg. of the Radiation Protection and Shielding Division*, Santa Fe, New Mexico, April 14–18, 2002, American Nuclear Society (2002).
36. M. A. COOPER and E. W. LARSEN, "Automated Weight Windows for Global Monte Carlo Particle Transport Calculations," *Nucl. Sci. Eng.*, **137**, *1*, 1 (2001); https://doi.org/10.13182/NSE00-34.
37. M. M. MIFTEN and E. W. LARSEN, "The Quasi-Diffusion Method for Solving Transport Problems in Planar and Spherical Geometries," *Transp. Theory Stat. Phys.*, **22**, *2–3*, 165 (1993); http://www.tandfonline.com/doi/abs/10.1080/00411459308203811.
38. V. Y. GOL'DIN, "A Quasi-Diffusion Method of Solving the Kinetic Equation," *USSR Comput. Math. Math. Phys.*, **4**, *6*, 136 (1964); http://www.sciencedirect.com/science/article/pii/0041555364900850 (current as of Dec. 7, 2018).
39. T. L. BECKER, A. B. WOLLABER, and E. W. LARSEN, "A Hybrid Monte Carlo-Deterministic Method for Global Particle Transport Calculations," *Nucl. Sci. Eng.*, **155**, *2*, 155 (2007); https://doi.org/10.13182/NSE07-A2653.
40. D. E. PEPLOW, E. D. BLAKEMAN, and J. C. WAGNER, "Advanced Variance Reduction Strategies for Optimizing Mesh Tallies in MAVRIC," *Trans. Am. Nucl. Soc.*, **97**, 595 (2007); http://www.researchgate.net/profile/John_Wagner10/publication/237784020_Advanced_Variance_Reduction_Strategies_for_Optimizing_Mesh_Tallies_in_MAVRIC/links/54cd206d0cf24601c08cce96.pdf (current as of Dec. 7, 2018).
41. J. C. WAGNER, E. D. BLAKEMAN, and D. E. PEPLOW, "Forward-Weighted CADIS Method for Global Variance Reduction," *Trans. Am. Nucl. Soc.*, **97**, 630 (2007); http://wp.ornl.gov/sci/nsed/rnsd/staff/Publications/WagnerPubs/Wagner_FW-CADIS_Nov2007_ANS-Trans.pdf (current as of Dec. 7, 2018).
42. J. C. WAGNER, E. D. BLAKEMAN, and D. E. PEPLOW, "Forward-Weighted CADIS Method for Variance Reduction of Monte Carlo Calculations of Distributions and Multiple Localized Quantities," *Proc. Int. Conf. Advances in Mathematics, Computational Methods, and Reactor Physics*, Saratoga Springs, New York, May 3–7, 2009, American Nuclear Society (2009).
43. J. C. WAGNER and S. W. MOSHER, "Forward-Weighted CADIS Method for Variance Reduction of Monte Carlo Reactor Analyses," *Trans. Am. Nucl. Soc.*, **103**, 342 (2010).
44. R. S. BAKER and E. W. LARSEN, "A 'Local' Exponential Transform Method for Global Variance Reduction in Monte Carlo Transport Problems," LA-UR-92-2349, Los Alamos National Laboratory (1993); http://www.osti.gov/scitech/biblio/10167411 (current as of Dec. 7, 2018).
45. A. J. VAN WIJK, G. VAN DEN EYNDE, and J. E. HOOGENBOOM, "An Easy to Implement Global Variance Reduction Procedure for MCNP," *Ann. Nucl.*

Energy, **38**, *11*, 2496 (2011); http://www.sciencedirect.com/science/article/pii/S0306454911003203 (current as of Dec. 7, 2018).

46. A. DAVIS and A. TURNER, "Comparison of Global Variance Reduction Techniques for Monte Carlo Radiation Transport Simulations of ITER," *Fusion Eng. Des.*, **86**, *9–11*, 2698 (2011); https://doi.org/10.1016/j.fusengdes.2011.01.059.
47. D. E. PEPLOW, "Comparison of Hybrid Methods for Global Variance Reduction in Shielding Calculations," *Trans. Am. Nucl. Soc.*, **107**, 512 (2012).
48. K. A. VAN RIPER, T. J. URBATSCH, and P. D. SORAN, "AVATAR Automatic Variance Reduction in Monte Carlo Calculations," Los Alamos National Laboratory (1997); http://www.osti.gov/scitech/biblio/527548 (current as of Dec. 7, 2018).
49. R. E. ALCOUFFE, "THREEDANT: A Code to Perform Three-Dimensional, Neutral Particle Transport Calculations," Los Alamos National Laboratory (1994).
50. E. T. JAYNES, "Information Theory and Statistical Mechanics," *Phys. Rev.*, **106**, *4*, 620 (1957); http://journals.aps.org/pr/abstract/10.1103/PhysRev.106.620 (current as of Dec. 7, 2018).
51. E. T. JAYNES, "Information Theory and Statistical Mechanics. II," *Phys. Rev.*, **108**, *2*, 171 (1957); http://journals.aps.org/pr/abstract/10.1103/PhysRev.108.171 (current as of Dec. 7, 2018).
52. O. B. MOSKALEV, "The Reconstruction of a Positive Function from Its Finite Fourier Series," *Transp. Theory Stat. Phys.*, **22**, *2–3*, 347 (1993); http://www.tandfonline.com/doi/pdf/10.1080/00411459308203818.
53. W. F. WALTERS and T. A. WAREING, "A Nonlinear Positive Method for Solving the Transport Equation on Course [*sic*]Meshes," Los Alamos National Laboratory (1994); http://www.iaea.org/inis/collection/NCLCollectionStore/_Public/25/048/25048476.pdf (current as of Dec. 7, 2018).
54. W. F. WALTERS and T. A. WAREING, "An Accurate, Strictly-Positive, Nonlinear Characteristic Scheme for the Discrete-Ordinate Equations," *Transp. Theory Stat. Phys.*, **25**, *2*, 197 (1996); http://www.tandfonline.com/doi/abs/10.1080/00411459608204836.
55. D. E. PEPLOW, S. W. MOSHER, and T. M. EVANS, "Consistent Adjoint Driven Importance Sampling Using Space, Energy, and Angle," ORNL/TM-2012/7, Oak Ridge National Laboratory (2012).
56. M. MUNK, "FW/CADIS-Ω: An Angle-Informed Hybrid Method for Neutron Transport," PhD Dissertation, University of California, Berkeley (2017); https://escholarship.org/uc/item/26c5k0tq (current as of Dec. 7, 2018).
57. K. L. ROWLAND et al., "Assessment of the Lagrange Discrete Ordinates Equations for Three-Dimensional Neutron Transport," *Nucl. Sci. Eng.*, **193**, 233 (2019); https://doi.org/10.1080/00295639.2018.1509569.
58. K. ROWLAND, "Advanced Quadrature Selection for Monte Carlo Variance Reduction," PhD Thesis, University of California, Berkeley (2018).
59. H. C. GUPTA and S. R. DWIVEDI, "Sampling of Scattering Angle in Deep-Penetration Monte Carlo," *Ann. Nucl. Energy*, **12**, *4*, 213 (1985); https://doi.org/10.1016/0306-4549(85)90047-7.
60. S. DWIVEDI, "A New Importance Biasing Scheme for Deep-Penetration Monte Carlo," *Ann. Nucl. Energy*, **9**, *7*, 359 (1982); https://doi.org/10.1016/0306-4549(82)90038-X.
61. T. UEKI and E. W. LARSEN, "A Kinetic Theory for Nonanalog Monte Carlo Particle Transport Algorithms: Exponential Transform with Angular Biasing in Planar-Geometry Anisotropically Scattering Media," *J. Comput. Phys.*, **145**, *1*, 406 (1998); http://www.sciencedirect.com/science/article/pii/S0021999198960399 (current as of Dec. 7, 2018).
62. J. S. HENDRICKS and L. L. CARTER, "Anisotropic Angle Biasing of Photons," *Nucl. Sci. Eng.*, **89**, *2*, 118 (1985); https://doi.org/10.13182/NSE85-A18186.
63. J. P. BOTH, J. C. NIMAL, and T. VERGNAUD, "Automated Importance Generation and Biasing Techniques for Monte Carlo Shielding Techniques by the TRIPOLI-3 Code," *Prog. Nucl. Energy*, **24**, *1*, 273 (1990); http://www.sciencedirect.com/science/article/pii/0149197090900468 (current as of Dec. 7, 2018).
64. S. A. TURNER and E. W. LARSEN, "Automatic Variance Reduction for Three-Dimensional Monte Carlo Simulations by the Local Importance Function Transform—I: Analysis," *Nucl. Sci. Eng.*, **127**, *1*, 22 (1997); https://doi.org/10.13182/NSE127-22.
65. S. A. TURNER and E. W. LARSEN, "Automatic Variance Reduction for Three-Dimensional Monte Carlo Simulations by the Local Importance Function Transform—II: Numerical Results," *Nucl. Sci. Eng.*, **127**, *1*, 36 (1997); https://doi.org/10.13182/NSE127-36.
66. K. P. KEADY and E. W. LARSEN, "A Modified Monte Carlo Local Importance Function Transform Method," *Nucl. Eng. Des.*, **295**, 625 (2015); https://doi.org/10.1016/j.nucengdes.2015.07.021.
67. T. L. BECKER and E. W. LARSEN, "A General Transform for Variance Reduction in Monte Carlo Simulations," *Proc. Int. Conf. Mathematics and Computational Methods Applied to Nuclear Science and Engineering*, Rio de Janeiro, Brazil (2011).
68. C. J. SOLOMON et al., "A Priori Deterministic Computational-Cost Optimization of Weight-Dependent Variance-Reduction Parameters for Monte Carlo Neutral-Particle Transport," *Nucl. Sci. Eng.*, **176**, *1*, 1 (2014); https://doi.org/10.13182/NSE12-81.

69. J. A. KULESZA et al., "Performance Assessment of Cost-Optimized Variance Reduction Parameters in Radiation Shielding Scenarios," *Proc. Int. Conf. Mathematics and Computational Methods Applied to Nuclear Science and Engineering*, Jeju, Korea, April 16–20, 2017, American Nuclear Society (2017); https://www.kns.org/files/int_paper/paper/MC2017_2017_2/P108S02-03KuleszaJ.pdf (current as of Dec. 7, 2018).

70. J. KULESZA, "Cost-Optimized Automated Variance Reduction for Highly Angle-Dependent Radiation Transport Analyses," Dissertation, University of Michigan (2018).

71. S. W. MOSHER et al., "Automated Weight-Window Generation for Threat Detection Applications Using ADVANTG," *Proc. Int. Conf. Mathematics, Computational Methods, and Reactor Physics (M&C 2009)*, Saratoga Springs, New York, May 3–7, 2009, American Nuclear Society (2009); http://www.northeastern.edu/sds/RadiationsensorData.pdf (current as of Dec. 7, 2018).

72. T. M. EVANS et al., "Denovo: A New Three-Dimensional Parallel Discrete Ordinates Code in SCALE," *Nucl. Technol.*, **171**, *2*, 171 (2010); https://doi.org/10.13182/NT171-171.

73. E. SOMASUNDARAM and T. S. PALMER, "Implementation of Hybrid Variance Reduction Methods in a Multi Group Monte Carlo Code for Deep Shielding Problems," *Proc. Int. Conf. Mathematics and Computational Methods Applied to Nuclear Science and Engineering (M&C 2013)*, Sun Valley, Idaho, May 5–9, 2013, American Nuclear Society (2013); http://www.osti.gov/scitech/biblio/22212710 (current as of Dec. 7, 2018).

74. D. S. LUCAS et al., "Applications of the 3-D Deterministic Transport Attila for Core Safety Analysis," *Proc. Americas Nuclear Energy Symp. 2004*, Miami Beach, Florida, October 3–6, 2004; https://digital.library.unt.edu/ark:/67531/metadc785664/ (current as of Dec. 7, 2018).

75. J. SWEEZY et al., "Automated Variance Reduction for MCNP Using Deterministic Methods," *Radiat. Prot. Dosim.*, **116**, *1–4*, 508 (2005); http://rpd.oxfordjournals.org/content/116/1-4/508.short.(current as of Dec. 7, 2018).

76. R. E. ALCOUFFE et al., "PARTISN Manual," LA-UR-02-5633, Los Alamos National Laboratory (2002).

77. G. RADULESCU et al., "Dose Rate Analysis of As-Loaded Spent Nuclear Fuel Casks," Oak Ridge National Laboratory (2013).

78. Y. F. CHEN et al., "Surface Dose Rate Calculations of a Spent-Fuel Storage Cask by Using MAVRIC and Its Comparison with SAS4 and MCNP," *Nucl. Technol.*, **175**, *1*, 343 (2011); https://doi.org/10.13182/NT11-A12306.

79. R. J. SHEU et al., "Dose Evaluation for an Independent Spent-Fuel Storage Installation Using MAVRIC," *Nucl. Technol.*, **175**, *1*, 335 (2011); https://doi.org/10.13182/NT11-A12305.

80. S. W. MOSHER, "A New Version of the ADVANTG Variance Reduction Generator," Oak Ridge National Laboratory(2010); http://www.osti.gov/scitech/biblio/978283 (current as of Dec. 7, 2018).

81. A. M. BEVILL and S. W. MOSHER, "A New Source Biasing Approach in ADVANTG," Oak Ridge National Laboratory (2012); http://www.osti.gov/scitech/biblio/1044655 (current as of Dec. 7, 2018).